Molecular Therapy
Nucleic Acids
Original Article

Translation of Angiotensin-Converting Enzyme 2 upon Liver- and Lung-Targeted Delivery of Optimized Chemically Modified mRNA

Eva Schrom,[1,2] Maja Huber,[2] Manish Aneja,[2] Christian Dohmen,[2] Daniela Emrich,[2] Johannes Geiger,[2] Günther Hasenpusch,[2] Annika Herrmann-Janson,[2] Verena Kretzschmann,[2] Olga Mykhailyk,[2] Tamara Pasewald,[2] Prajakta Oak,[3] Anne Hilgendorff,[3] Dirk Wohlleber,[4] Heinz-Gerd Hoymann,[5] Dirk Schaudien,[5] Christian Plank,[2,4] Carsten Rudolph,[1,2] and Rebekka Kubisch-Dohmen[2]

[1]Department of Pediatrics, LMU Munich, 80802 Munich, Germany; [2]Ethris GmbH, 82152 Planegg, Germany; [3]Comprehensive Pneumology Center, Institute of Lung Biology and Disease, Helmholtz Zentrum Munich, 81377 Munich, Germany; [4]Institute of Molecular Immunology and Experimental Oncology, TU Munich, 81675 Munich, Germany; [5]Fraunhofer Institute for Toxicology and Experimental Medicine, 30625 Hannover, Germany

Changes in lifestyle and environmental conditions give rise to an increasing prevalence of liver and lung fibrosis, and both have a poor prognosis. Promising results have been reported for recombinant angiotensin-converting enzyme 2 (ACE2) protein administration in experimental liver and lung fibrosis. However, the full potential of ACE2 may be achieved by localized translation of a membrane-anchored form. For this purpose, we advanced the latest RNA technology for liver- and lung-targeted ACE2 translation. We demonstrated in vitro that transfection with ACE2 chemically modified messenger RNA (cmRNA) leads to robust translation of fully matured, membrane-anchored ACE2 protein. In a second step, we designed eight modified ACE2 cmRNA sequences and identified a lead sequence for in vivo application. Finally, formulation of this ACE2 cmRNA in tailor-made lipidoid nanoparticles and in lipid nanoparticles led to liver- and lung-targeted translation of significant amounts of ACE2 protein, respectively. In summary, we provide evidence that RNA transcript therapy (RTT) is a promising approach for ACE2-based treatment of liver and lung fibrosis to be tested in fibrotic disease models.

INTRODUCTION

Fibrotic diseases are major causes of mortality and morbidity worldwide, leading to a serious economic burden and challenges for health services.[1,2] Fibrosis is caused by repetitive noxious stimuli leading to cell stress, injury, and apoptosis, causing organ dysfunction and ultimately organ failure.[3,4] Fibrosis can affect nearly every organ, with liver and lung fibrosis showing a rising prevalence due to lifestyle changes or unfavorable environmental conditions.[5–7] Currently, there are several treatment options under evaluation for liver and lung fibrosis; however, these have had limited therapeutic success, raising the need for new therapeutic approaches.[8–10] Investigations of the underlying mechanisms of fibrotic diseases showed that dysregulation of the organ-specific renin-angiotensin system (RAS) plays a critical role in disease onset by triggering excessive pro-inflammatory and pro-fibrotic signaling.[1]

Angiotensin-converting enzyme 2 (ACE2) is a family member of the RAS and acts as a metallo-carboxypeptidase cleaving angiotensin II (AngII) to Ang-(1-7). AngII acts on the AngII type I receptor (AT1R), leading to pro-inflammatory and pro-fibrotic signaling, while Ang-(1-7) acts on the Mas oncogenic receptor (Mas receptor), leading to anti-inflammatory and anti-fibrotic signaling. Thus, ACE2 can shift the RAS balance by reducing the amount of AngII and at the same time increasing the amount of Ang-(1-7) molecules. Therefore, ACE2 not only re-establishes the physiologic balance of the RAS, but it also clearly shifts it toward resolution of inflammation and fibrosis.[11–13]

ACE2 levels are markedly increased in patients with liver fibrosis as well as in experimental models, which may be due to a counter-regulatory response to RAS upregulation.[14] *ACE2* knockout studies revealed that the loss of ACE2 leads to exacerbation of liver injury, which can be attenuated by administration of recombinant ACE2[15] or by adeno-associated *ACE2* gene therapy.[16] Similar therapeutic effects were shown by administration of Ang-(1-7)[17] and as a side-effect of AngII receptor blocker (ARB) therapy.[18,19] Interestingly, unlike observations in liver fibrosis, ACE2 levels are markedly decreased in lung tissue from patients suffering from idiopathic pulmonary fibrosis (IPF).[20] In murine models, two studies showed that intraperitoneal injection of exogenous ACE2 protein in bleomycin-induced lung

Received 3 January 2017; accepted 7 April 2017;
http://dx.doi.org/10.1016/j.omtn.2017.04.006.

Correspondence: Rebekka Kubisch-Dohmen, Ethris GmbH, Semmelweisstr. 3, 82152 Planegg, Germany.
E-mail: kubisch@ethris.com
Correspondence: Carsten Rudolph, Ethris GmbH, Semmelweisstr. 3, 82152 Planegg, Germany.
E-mail: rudolph@ethris.com

fibrosis led to re-establishment of local ACE2 levels and reduced levels of lung injury.[21,22] The same protective effect of ACE2 could be shown in a bleomycin-induced mouse model by intratracheal administration of lentiviral packaged Ang-(1–7) fusion gene or ACE2 cDNA.[23]

RNA transcript therapy (RTT) has gained substantial attention as a newly evolving therapeutic approach. mRNA exerts its function in the cytoplasm, leading to high and reliable transfection efficiency in proliferating as well as quiescent cells without the risk of insertional mutagenesis faced by viral vectors or plasmid DNA (pDNA). In comparison to recombinant protein therapy, RTT is not limited to secreted proteins, making it an interesting alternative for translation of intracellular or membrane-bound protein. Due to enzymatic mRNA degradation mechanisms in the cytoplasm, protein translation is controllable, as it is naturally self-limited.[24–26] Many of the initial obstacles of mRNA therapy, such as RNA instability and immunogenicity, have been solved, offering today a repertoire of techniques for designing chemically modified mRNA (cmRNA) with tailor-made pharmacodynamic properties.[27–31] However, clinical application of RTT is still at a pre-clinical stage, owing to challenges such as cell- or organ-specific delivery or the complexity of mRNA pharmacology.[26]

As previously stated, promising results of ACE2 therapy in experimental liver and lung fibrosis have been reported.[14–17,21–23] In human clinical trials, the safety and tolerability of systemically applied recombinant ACE2 was shown.[32,33] However, localized translation of membrane-anchored ACE2 may be even more favorable. This may be achieved with recent advances in cmRNA technology.[34–36] Therefore, the objective of this study was to establish robust ACE2 translation from cmRNA in the liver or lung, respectively. First, we performed an in vitro validation of ACE2 cmRNA translation, protein activity, and integrity. In a second step, we designed eight different cmRNA sequences and screened them in cell culture to identify the optimal cmRNA composition for sustained protein translation and activity in liver and lung cells. Finally, this lead candidate was formulated for liver- or lung-specific delivery, which led to increased translation of ACE2 protein selectively in these organs.

RESULTS

ACE2 cmRNA Is Successfully Transfected and Translated In Vitro

In our first set of experiments, we investigated RNA delivery of in vitro-transcribed chemically modified ACE2 RNA and its successful translation into ACE2 protein. As a generic test system, we chose HEK293 human embryonic kidney cells, which are frequently used for transient transfection experiments. With the aim of liver- and lung-targeted protein translation in subsequent in vivo studies, we selected A549 alveolar epithelial cells (AECs) and HepG2 hepatoma cells as representative human cell lines and hepatocytes and lung fibroblasts as representative primary murine cells.

First, all cells were screened for their endogenous levels of ACE2 mRNA (Figure S1). Endogenous levels in pulmonary cells were either not detectable (as in the case of lung fibroblasts) or were at detection limit (in the case of A549 cells). All other cells showed moderate levels of ACE2 mRNA relative to three reference genes. Cellular uptake of cmRNA after transfection was analyzed by real-time PCR (Figure 1A). cmRNA uptake was quantified against a set of reference genes (which were not affected by the experimental conditions; data not shown). 24 hr after transfection, ACE2 cmRNA was successfully taken up in all ACE2 cmRNA-treated samples, while no ACE2 cmRNA could be detected in control cmRNA or untransfected samples. In a next step, we aimed at verifying whether ACE2 cmRNA is successfully translated into ACE2 protein. First, ACE2 protein abundance after transfection was analyzed by western blot. For this purpose, A549, HepG2, and HEK293 cells were transfected with two doses of ACE2 cmRNA, respectively. All three cell lines showed clear dose-dependent expression levels for ACE2 protein (Figure 1B). Likewise, transfection of primary liver and lung cells with ACE2 cmRNA also led to clearly detectable ACE2 protein levels. Second, enzymatic activity of ACE2 protein was analyzed by an ACE2 activity assay (Figure 1C). All ACE2 cmRNA-transfected samples showed a significant induction in ACE2 activity relative to untransfected samples. These findings demonstrate that ACE2 cmRNA transfection leads to translation of an enzymatically active protein in liver and lung cells.

During Post-translational Modification, ACE2 Is Glycosylated and Integrated into the Plasma Membrane

ACE2 is a typical type I integral membrane protein with the core domain located at the extracellular surface. The extracellular domain is flanked by a signal peptide followed by the catalytic domain, which has several glycosylation sites.[37] It was crucial for our in vivo studies to guarantee a locally expressed membrane-bound version of ACE2 protein; therefore, we specifically investigated post-translational modifications (e.g., glycosylation and intramolecular disulfide bonds) with regard to these biological properties. N-linked glycosylation is pivotal for proper folding, assembly, and trafficking of membrane proteins. Therefore, we investigated whether cmRNA-derived ACE2 protein is glycosylated and correctly integrated into the plasma membrane. Cells transfected with ACE2 cmRNA produced an ACE2 protein with a size of 120 kDa, corresponding to the mature, fully glycosylated form of the protein.[38] The glycosylation process was successfully inhibited by treating cells with tunicamycin, an inhibitor of N-linked glycosylation.[39] Retrospective deglycosylation of mature ACE2 protein by enzymatic deglycosylation resulted in the same protein size as inhibition of glycosylation, confirming full protein glycosylation (Figure 2A). Additionally, the formation of disulfide bonds is shown in Figure S8. To verify correct protein integration and expression on the cell surface, ACE2 cmRNA-transfected cells were stained with anti-ACE2 antibody recognizing the ACE2 core domain located on the cell surface. Cells were then analyzed by flow cytometry (Figures 2B and 2C). In all three cell lines, ACE2 cmRNA-transfected samples showed a clear increase in ACE2 translation relative to untransfected samples. To localize

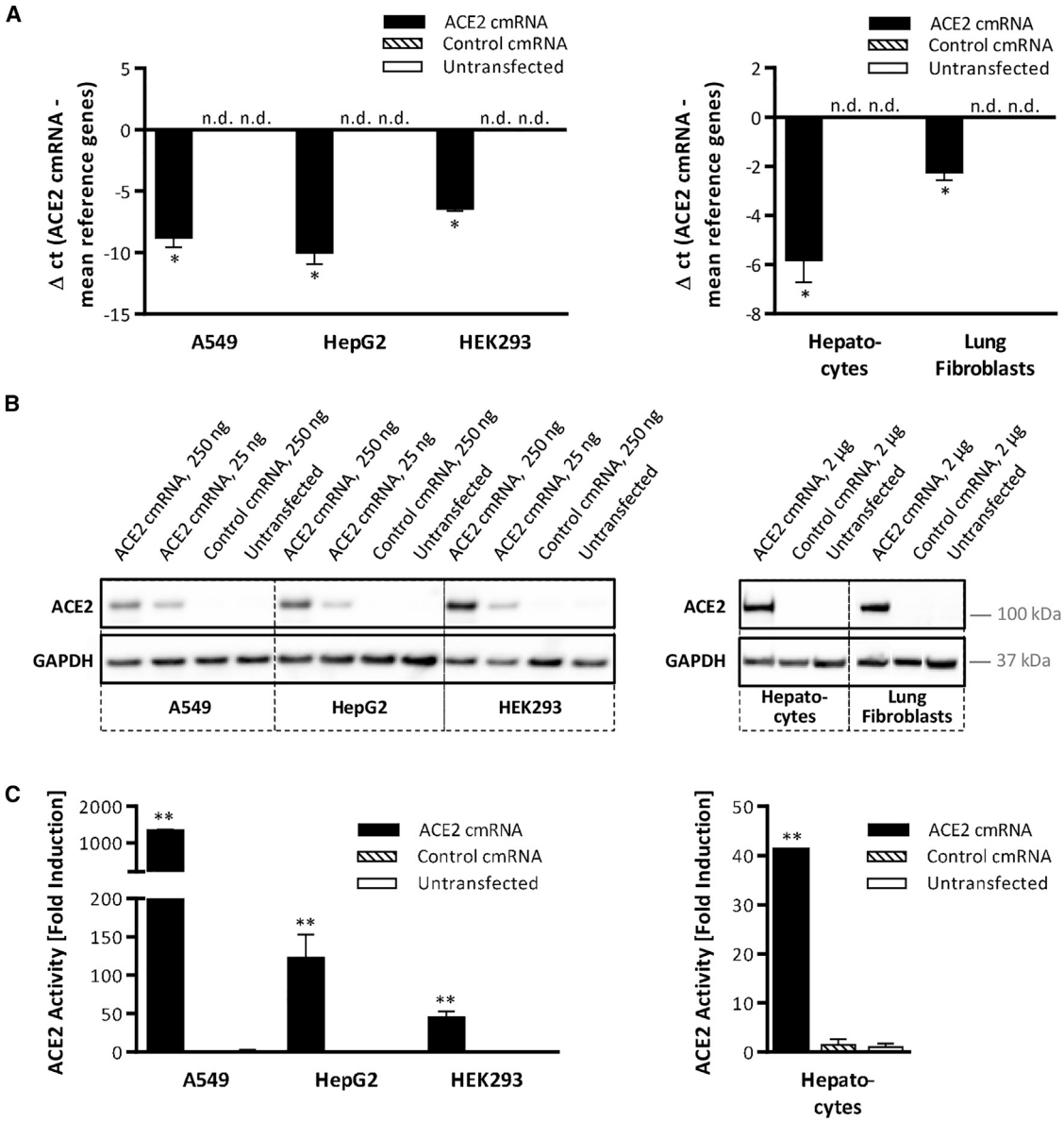

Figure 1. Detection of ACE2 cmRNA and Encoded Protein in Different Cell Types

(A) 24 hr after transfection, total RNA of five different cell types was collected and transcribed into first-strand cDNA. The relative expression of ACE2 cmRNA against a panel of reference genes was determined by real-time qPCR. Means ± SEM are shown (n = 3). *$p < 0.05$; **$p < 0.01$. (B) Cells were lysed 24 hr after transfection and the cell lysate was analyzed by western blot with GAPDH as the loading control. (C) A fraction of the cell lysate was used for determination of ACE2 activity. For all experiments, luciferase cmRNA was used as the control cmRNA. Fold induction of ACE2 activity relative to untransfected samples is depicted. **$p < 0.01$.

cmRNA-derived protein, A549 and HepG2 cells were transfected with ACE2 cmRNA and ACE2 protein was visualized by fluorescence staining (HepG2 and A549 cells in Figures 2D and S3, respectively). In both cell lines, samples transfected with ACE2 cmRNA stained positive for ACE2 protein, while transfection with control cmRNA showed only a weak background signal in HepG2 cells. In light of potential future therapeutic applications for lung and liver fibrosis, endogenous levels of ACE2 protein are not sufficient to prevent disease onset and progress; hence, strong ACE2 translation is pivotal. The immunocytochemical images revealed ACE2 protein localization throughout the cytoplasm and on the plasma membrane. The accumulations found throughout the cytoplasm showed a dotted pattern, indicating protein enrichment in vesicular structures probably involved in protein maturation or trafficking to the plasma membrane. The presence of ACE2 protein at the plasma membrane was indicated by co-localization of

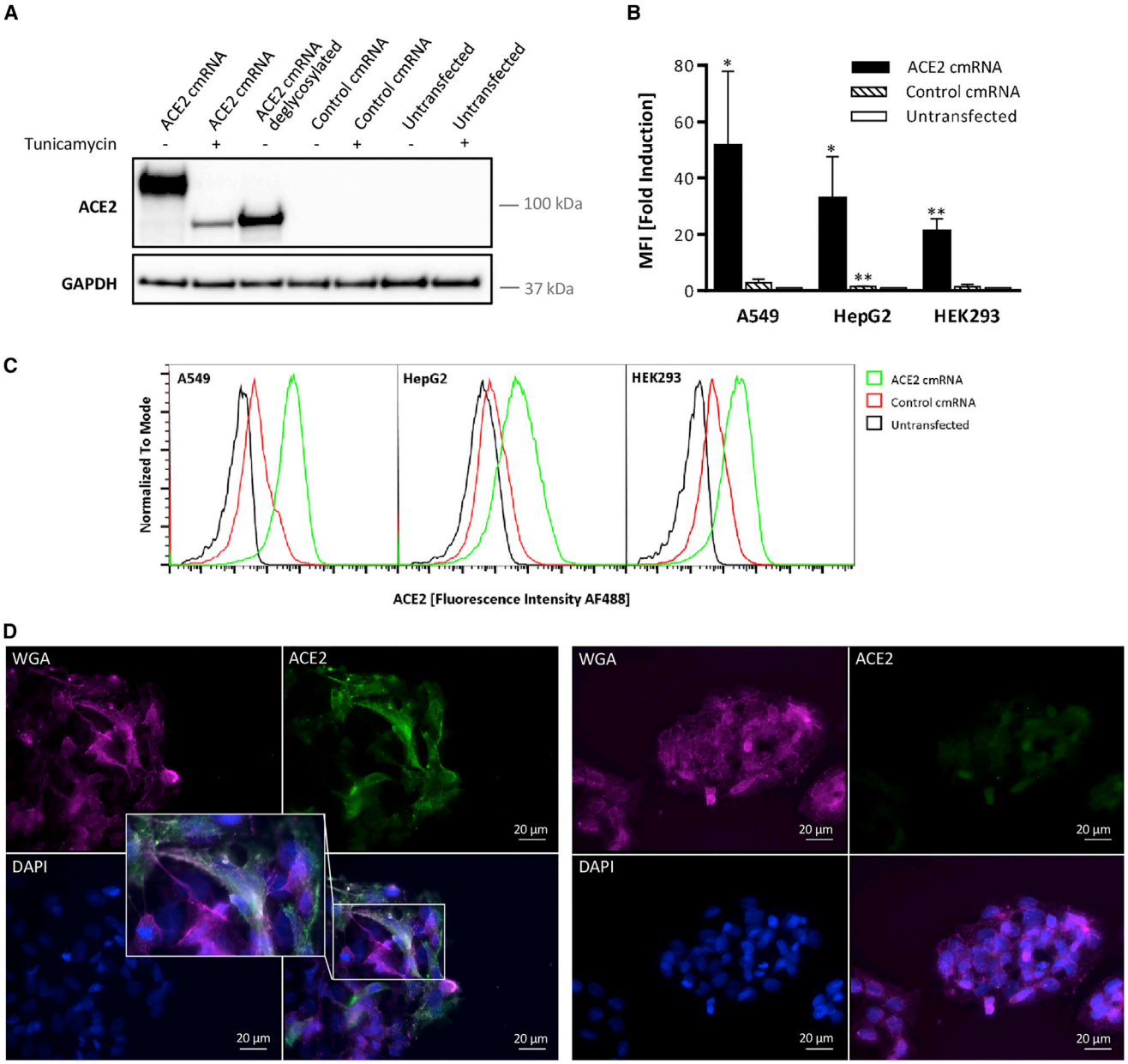

Figure 2. Post-translational Processing and Localization of ACE2 cmRNA

(A) Prior to transfection, A549 cells were treated with tunicamycin. 24 hr after transfection, cells were lysed and the cell lysate was analyzed by western blot. (B) Cells were transfected with ACE2 cmRNA and were stained 24 hr after transfection for extracellular ACE2 protein expression, detected with Alexa Fluor (AF488)-conjugated secondary antibody. Samples were analyzed by FACS. Fold change was calculated against untransfected samples using the Student's t test. *$p < 0.05$; **$p < 0.01$. Mean fluorescence intensity (MFI) is shown. (C) Representative histograms for each cell line. (D) Immunofluorescence staining for ACE2 protein in HepG2 24 hr after transfection with ACE2 cmRNA (left panel) and control cmRNA (right panel). Green, ACE2; blue, nucleus; violet, cell membrane. For all experiments, luciferase cmRNA was used as the control cmRNA. WGA, wheat germ agglutinin. Means ± SD are shown.

ACE2 with wheat germ agglutinin, a plasma membrane marker (white staining patterns in overlay images). Taken together, we could prove that ACE2 cmRNA-derived protein undergoes biological post-translational modifications leading to correct integration into the plasma membrane.

Codon-Optimized ACE2 cmRNA with Human α-Globin 5′ UTR Leads to Enhanced cmRNA Stability and ACE2 Protein Translation

After having successfully verified that the sequence of ACE2 cmRNA leads to the translation of an active membrane-bound form of ACE2

Table 1. Half-Life of ACE2 cmRNA Sequences

					Codon Optimized			
	Natural	Minimal	hαG	CYBA	Natural	Minimal	hαG	CYBA
A549								
Half-life (hr)	7.65	5.09	6.77	7.99	10.29	11.35	13.30	11.10
95% confidence interval	6.01–10.54	4.69–5.55	6.52–7.03	5.71–13.35	9.27–11.57	8.23–18.27	9.44–22.53	8.48–16.08
HepG2								
Half-life (hr)	7.22	5.66	5.66	9.29	6.95	7.81	9.16	10.86
95% confidence interval	5.35–11.11	5.24–6.16	5.11–6.35	7.83–11.42	5.66–9.00	6.86–9.07	6.95–13.42	7.71–18.37

protein, we wanted to further optimize the sequence for strong protein translation. Therefore, we designed eight different ACE2 cmRNA sequences, sharing the same open reading frame (ORF) encoding ACE2, a C1-m7G cap, and a poly(A) tail of ~120 nucleotides, which was found to be the optimal length.[40] In addition to the natural ACE2 mRNA sequence, we introduced three different modifications of the UTRs known for a high level of protein translation[41–43]: namely, a minimal 5′ UTR, a human alpha globin (hαG) 5′ UTR, and a cytochrome *b*-245 alpha poly-peptide (CYBA) 5′ with 3′ UTR. For all four sequences, we designed one natural version and one codon-optimized version of the ORF.

First, we were interested in the effect of the cmRNA modifications on intracellular ACE2 cmRNA stability. Overall, cmRNA followed a degradation pattern of an exponential one-phase decay (Figure S2). The RNA of all sequences was detectable 72 hr after transfection. Overall, codon optimization slowed the rate of cmRNA degradation, leading to higher levels of cmRNA at later time points. The only exception was the codon-optimized natural ACE2 sequence, which had the highest number of non-codon-optimized nucleotides in its sequence due to the long natural 5′ and 3′ UTR regions. Based on these data, the half-life for each sequence was calculated for the decay phase (Table 1). In A549 cells, all codon-optimized sequences showed an extended half-life compared to native sequences. In HepG2 cells, codon optimization led to a prolonged half-life for hαG and minimal cmRNA sequences. Looking at ACE2 translation efficiency, codon optimization led to stronger protein translation in both cell lines for up to 144 hr (A549 and HepG2 cells in Figure 3A, left and right panels, respectively). The strongest protein translation was observed for codon-optimized hαG cmRNA, followed by codon-optimized minimal cmRNA. Despite the extended half-life of codon-optimized CYBA cmRNA, ACE2 protein abundance could not reach the levels of codon-optimized minimal and hαG cmRNA. Data obtained by western blot were confirmed by an ACE2 activity assay (A549 and HepG2 cells in Figure 3B, left and right panels, respectively). In both cell lines, ACE2 enzymatic activity was significantly increased for samples transfected with codon-optimized hαG cmRNA and codon-optimized minimal cmRNA relative to untransfected samples. Based on these results, codon-optimized minimal and codon-optimized hαG cmRNA were identified as the best performing sequences with regard to cmRNA stability, protein translation, and kinetics. As the codon-optimized hαG cmRNA sequence showed a slightly longer half-life than the minimal sequence, it was used in all subsequent in vivo studies.

ACE2 cmRNA Can Be Selectively Targeted to the Liver and Lung and Shows Strong ACE2 Protein Translation

Dysregulation of the local RAS contributes significantly to inflammation and fibrosis,[44,45] a process that can best be counterbalanced by specific ACE2 translation in the affected organs. For the purpose of liver-targeted cmRNA delivery, we chose lipoplexes (referred to as the liver lipidoid formulation [LLF] in the following) as described by Jarzębińska et al.[35] The liver specificity of LLF was first confirmed in a formulation with firefly luciferase cmRNA. A 1 mg/kg dose of this formulation was administered intravenously to mice and luciferase protein activity was measured 6 hr after administration. All animals showed strong and selective cmRNA uptake in the liver, without signals in other organs (Figures 4A and 4B). Luciferase protein expression in the liver clearly mirrored the blood flow through the organ, thereby reflecting lipoplex distribution after intravenous injection (Figures 4C and S7). Strong protein enrichment was observed close to the portal region, where afferent vessels enter the liver, with a gradual decrease toward the efferent central vein. After we successfully verified targeted and selective enrichment of LLF-complexed cmRNA and protein translation in the liver, we formulated two doses of ACE2 cmRNA (4 and 2 mg/kg) and a single dose (2 mg/kg) of control cmRNA in LLF for intravenous injection in mice. 6 hr after treatment, in situ hybridization of livers from ACE2 cmRNA-treated animals showed cmRNA uptake by hepatocytes and detection of cmRNA in liver sinusoids throughout the liver sample in a more or less homogeneous pattern (Figures 4D and S7). These results were confirmed by real-time PCR, showing significant ACE2 cmRNA in liver homogenates of these animals (Figure 4E). Quantification of deposited ACE2 cmRNA showed a clear dose-dependent uptake of 0.032 ± 0.007 ng ACE2 cmRNA/μg total RNA for a 4-mg/kg dose and 0.016 ± 0.002 ACE2 cmRNA/μg total RNA for a 2-mg/kg dose. There was no ACE2 cmRNA detected in the control group. ACE2 cmRNA was successfully translated, as shown in western blot analysis (Figure 4F) by a clear increase in ACE2 protein abundance in the ACE2 treatment groups. Glycosylation was shown by enzymatic deglycosylation of liver homogenates, inducing a shift in protein size indicative for the active glycosylation process in vivo. In

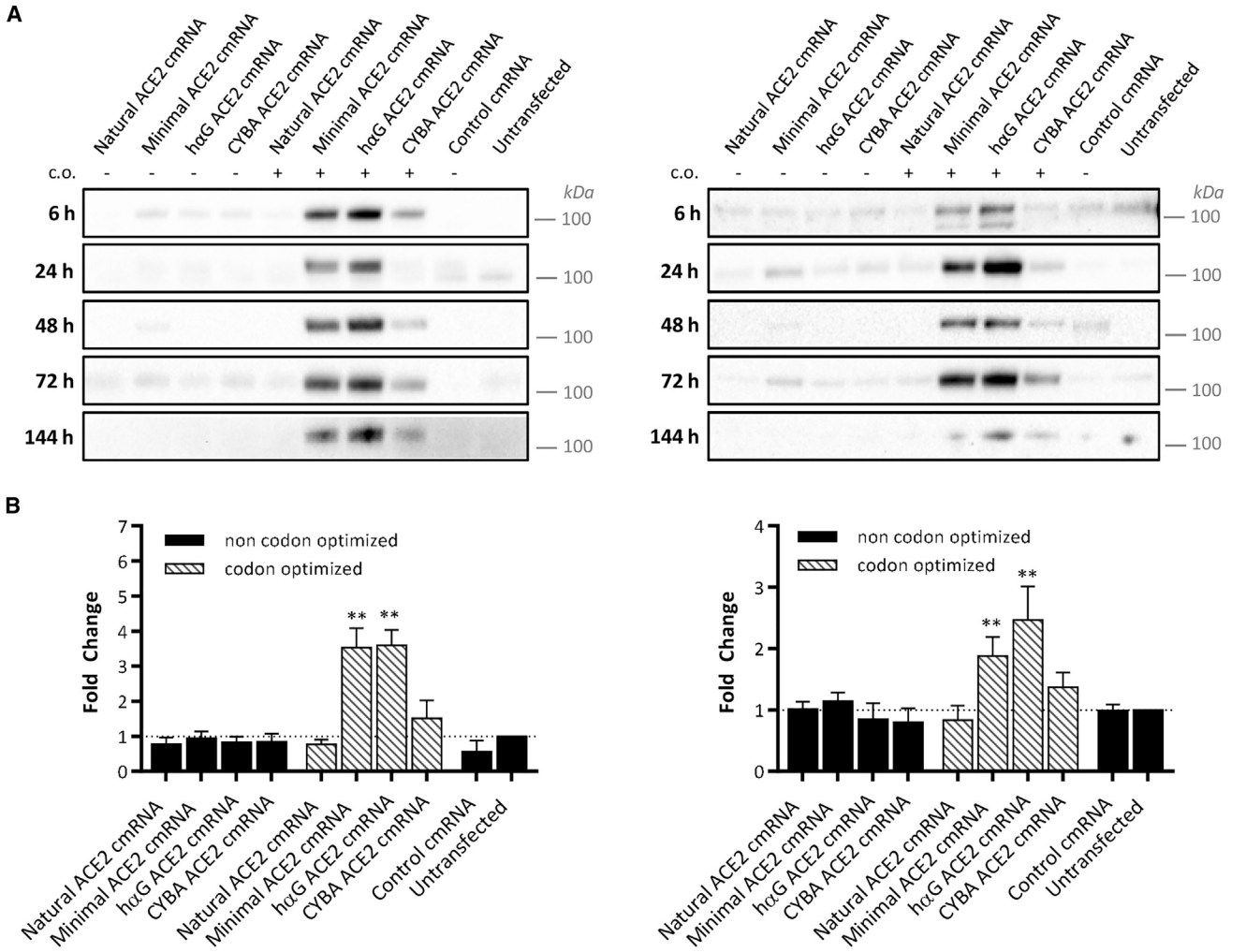

Figure 3. Screening of ACE2 cmRNA Sequences

(A) A549 (left panel) and HepG2 (right panel) cells were transfected with eight different ACE2 cmRNA sequences and lysed after 6 hr, 24 hr, 48 hr, 72 hr, and 144 hr. ACE2 protein translation was analyzed by western blot. (B) 24 hr after transfection, ACE2 activity assay was performed for A549 (left panel) and HepG2 (right panel) cells. Fold induction of ACE2 activity relative to untransfected samples is depicted. For all experiments, EGFP cmRNA was used as the control cmRNA. Data were analyzed by one-way ANOVA. **$p < 0.01$. c.o., codon optimized. Means ± SD are shown.

the ACE2 activity assay (Figure 4G), significantly higher protein activity was detected in ACE2-transfected liver samples than in the control group showing endogenous ACE2 baseline activity.

For the purpose of pulmonary cmRNA delivery, we developed a novel proprietary lipid formulation especially designed for lung-targeted cmRNA delivery by intravenous injection (referred to as the pulmonary lipid formulation [PLF] in the following). First, the lung targeting of the formulation was evaluated by intravenous application of luciferase cmRNA in PLF in mice at a dose of 1 mg/kg. 6 hr after injection, a strong luciferase signal was detected selectively in the lungs, whereas other organs did not show any signal (Figure 5A). After we identified PLF as a selective delivery agent for lung application, we formulated a mixture of 90% ACE2 cmRNA or 90% control cmRNA and 10% luciferase cmRNA in PLF. A 1-mg/kg dose of this formulation was administered intravenously to mice, while sham-treated animals received a single injection of PBS. After 6 hr, lung-specific delivery was confirmed by luciferase activity, which showed high levels in the lungs compared to other organs for all animals that received PLF formulations (Figure 5B). In situ hybridization of ACE2 cmRNA-treated animals showed a homogeneous distribution of positive-stained cells in the alveolar walls, which were interpreted to be type II and type I AECs (Figure 5C, left panel). Furthermore, single macrophages with cmRNA were found. Immunohistochemical stainings for ACE2 protein in ACE2-treated animals revealed multifocal membranous positive staining of cells located predominantly in the alveolar angles, most likely type II AECs or macrophages (Figure 5C, middle panel). In addition, ACE2 cmRNA-treated animals

showed positive cells in the alveolar walls with strong membrane and moderate cytoplasmic staining. The morphology of these cells is indicative of type I AECs. ACE2 protein abundance was increased in the ACE2 cmRNA-treated group, while control cmRNA and sham samples showed only endogenous ACE2 protein levels detected by western blot (Figure 5D). Overall, the application of cmRNA resulted in mild to moderate focally disseminated free alveolar erythrocytes (Figure 5C, right panel). Taken together, we have shown that intravenous administration of lipoplexes of a codon-optimized hαG ACE2 cmRNA in lipidoid nanoparticles (LLF) or PLF is able to strongly induce ACE2 protein translation selectively in the liver or lung.

DISCUSSION

Re-establishment of a well-balanced RAS is repeatedly shown to have promising therapeutic effects in the treatment of liver and lung fibrosis.[5,14,15,18,19,21–23,46] These effects may be further enhanced by local translation of ACE2 in affected organs, which is feasible with the latest cmRNA technology. In this study, we designed an optimized sequence of chemically modified ACE2 mRNA that leads to prominent ACE2 protein translation and activity in vitro and in vivo. Tailor-made lipidoid-based formulations of this optimized ACE2 cmRNA sequence led to ACE2 protein translation directly and selectively in the liver, while the lipid-based formulation for pulmonary delivery resulted in selective ACE2 translation in the lung using the same ACE2 cmRNA.

The RAS is a signaling cascade producing multiple biological active intermediates.[13] Initially, drug development was mainly focused on ACE inhibitors in the context of blood pressure regulation.[47] However, with increasing knowledge about the physiologic and pathologic properties of the biological intermediates further down the proteolytic cascade, AT1 receptor blockers, AT2 receptor agonists, recombinant ACE2 or ACE2 activators, and Ang-(1-7) analogs gained momentum.[48,49] With the exception of ACE2, the therapeutic purpose of all of these drugs was to either reduce pro-inflammatory and pro-fibrotic signaling through the AT1 receptor or to counterbalance AT1 receptor signaling by increased Mas receptor signaling. The effect of ACE2 regulators, however, is unique in the RAS, as they can achieve both. By cleaving AngII to Ang-(1-7), ACE2 reduces stimulation of AT1 receptor signaling and at the same time increases anti-inflammatory and anti-fibrotic signaling through the Mas receptor. The therapeutic effects of modulating the RAS by increased ACE2 signaling as just described were repeatedly shown for both liver and lung fibrosis. However, previous studies struggled with hurdles such as organ-specific delivery, controllable protein expression, and immunogenicity, among others. Post-translational modifications such as glycosylation are indispensable for full functionality of proteins subjected to such modifications, especially for ACE2 (a membrane-integrated protein), which cannot be guaranteed by recombinant protein therapy. These obstacles and requirements could potentially be solved by RTT; hence, we aimed at investigating the potential of ACE2 RTT. Thus, we designed an in vitro-transcribed chemically modified ACE2 mRNA sequence. This sequence was successfully tested in vitro for cellular cmRNA uptake and translation into enzymatically active protein in a generic test system (HEK293 cells), as well as in human and murine pulmonary and hepatocellular cells (Figure 1).

Administration of recombinant human ACE2 in experimental liver[15] and lung fibrosis[21] showed the first promising results. However, long-term effects on collagen deposition in the lung were considered questionable[20] and increased the need for local ACE2 delivery with greater efficacy, two requirements that are feasible with the latest advances in RTT. In addition, limited understanding of the physiological relevance of soluble ACE2 and a limited terminal half-life of 10 hr for recombinant ACE2 protein in humans[33] urged us to verify that cmRNA-derived ACE2 protein is processed to a stably expressed transmembrane protein. After we verified full protein glycosylation in vitro and in vivo (Figures 2A and 4F), a crucial step for protein trafficking and integration into the plasma membrane, we confirmed correct protein integration into the plasma membrane (Figures 2B–2D). In fluorescence stainings of ACE2 cmRNA-transfected cells, we could further observe ACE2 enrichment in vesicular structures, which may be part of the post-translational maturation machinery (Figures 2A, 2B, S3, and S4). However, a detailed analysis of all post-translational modifications relevant for ACE2 would be required for a complete assessment of the consensus between endogenous and ACE2 cmRNA-derived protein processing.

With potential future applications of ACE2 RTT in humans, careful consideration of the biochemical properties relating to its biological implications for pharmacokinetics and pharmacodynamics is required. Therefore, we optimized the ACE2 cmRNA sequence with regard to cmRNA stability, protein abundance, enzymatic activity, and translation kinetics. Based on our and other groups' work, we decided on a set of modifications that we considered most promising for our purpose. Cell type and cell state have a strong impact on how the cell reacts to variations in artificially introduced mRNA sequences.[42,50–52] The biological implications of these modifications need to be carefully evaluated. UTRs are key elements in the mRNA sequence for translation initiation, elongation, and termination as well as intracellular localization and mRNA stability,[53,54] all of which have a significant impact on final protein expression kinetics. Therefore, we designed sequences with three UTR modifications and a minimal 5′ UTR known for a high level of protein translation over an extended time period.[41–43] Codon optimization is another technique that is frequently used for strong protein translation. In this technique, translation rates are markedly increased by replacing rare codons with abundant codons without modifying the amino acid sequence of the encoded protein.[29,50] In addition, codon optimization reduces secondary structures of cmRNA, which may otherwise induce cellular immune reactions.[50] Therefore, for all four sequences, we designed one natural version and one codon-optimized version of the ORF. In our screen with A549 and HepG2 cells (Figure 3), we observed that codon optimization also led to an increased half-life for all cmRNA sequences in A549 cells, but not in HepG2 cells. Protein translation, however, was markedly increased

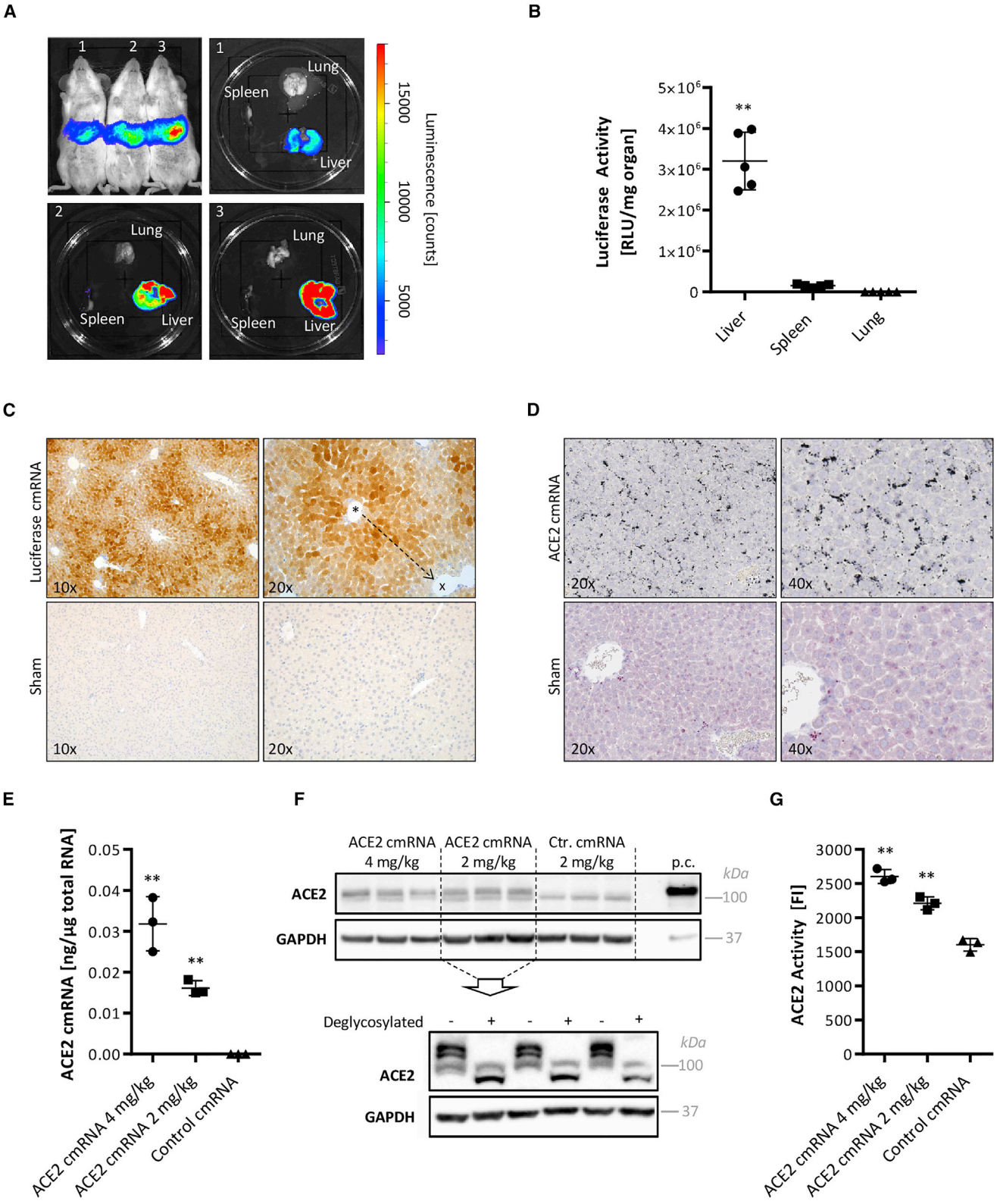

(legend on next page)

from 6 to 144 hr in both cell lines for codon-optimized sequences. We could further increase ACE2 protein translation and enzymatic activity by also replacing natural ACE2 UTRs with UTRs of strongly translated proteins. As the different UTRs did not affect the physical half-life of cmRNA (Table 1), we conclude that replacing UTRs did primarily increase translational efficiency, which is in line with previous findings.[41] For the purpose of liver- and lung-targeted application of ACE2 cmRNA, we could identify codon-optimized hαG ACE2 cmRNA as the best performing sequence. Furthermore, we observed that codon optimization of the hαG ACE2 cmRNA sequence led to reduced immunogenicity (Figures S4–S6), probably leading to a prolonged half-life and strong protein translation for up to 6 days in both cell lines.

Cell- and tissue-specific delivery of cmRNA is currently considered a major obstacle to overcome for RTT.[26] We could show that intravenous delivery of reporter cmRNA in LLF as described by Jarzębińska et al.[35] led to strong and liver-specific protein translation (Figures 4A and 4B). Immunohistochemical stainings indicate that intravenous application is a potent delivery mechanism for reaching a high number of hepatocytes, which was previously shown for delivery of small interfering RNA (siRNA) as well as mRNA.[26,55–58] The current understanding of the underlying mechanism is that lipoplexes enter the liver lobuli via fenestrated capillaries, which lack a diaphragm (unlike other types of capillaries). This makes them highly permeable for small molecules, and lipoplexes are easily taken up into the interstitium, where they are transported by ligand-based targeting or diffusion from the afferent to the efferent vessels.[56,57,59] This is visible in the histochemical stainings for luciferase protein showing a gradual decrease in protein abundance from the afferent to the efferent vessels (Figure 4C). This effect is observable throughout the whole organ, confirming the advantage of RTT over recombinant protein therapy and pDNA delivery—namely, to reach a large pool of cells even beyond physical barriers such as endothelium in both mitotic and non-mitotic cells, which was postulated previously by Matsui et al.[58] With the aim of shifting the local balance of the RAS toward resolution of fibrosis, we consider reaching hepatocytes, the most abundant cell type in the liver, a major achievement for strong translation of our target protein. In a second step, we applied the same delivery method to ACE2 cmRNA and saw markedly increased ACE2 protein translation and activity 6 hr after treatment (Figures 4F and 4G). Our in vitro findings (Figure 3) showed that ACE2 protein is detectable up to 5 days. If this expression pattern can be established in future in vivo models by RTT, ACE2 expression lies above levels reached by recombinant ACE2 therapy in humans[33] and below levels reached by adeno-associated viral ACE2 therapy in experimental models.[16] This emphasizes once more the advantages of RTT for a flexible dosing regimen for potential future clinical application.

Choosing the optimal administration route for lung-targeted cmRNA delivery requires careful consideration of the pathologic characteristics of the targeted disease. IPF is characterized by AEC apoptosis in response to repetitive microinjuries, and this effect is particularly evident adjacent to fibroblast foci.[60] Previous in vitro studies have shown that AECs produce more AngII in response to injury, while ACE2 mRNA is reduced at the same time. This makes AECs even more prone to injury and AngII-induced apoptosis.[20,61–63] We therefore consider delivering ACE2 cmRNA especially to these areas of epithelial cell death essential for therapeutic success. Due to scarring of the lung parenchyma, these areas are poorly ventilated, hindering the uptake of drugs via the airways. Looking at the vascularization of fibrotic lungs, it was shown that fibroblast foci themselves are poorly vascularized, while the adjacent non-fibrotic areas, where AEC apoptosis takes place, are highly vascularized.[64,65] Therefore, we hypothesized that it may be more effective to reach these areas via the pulmonary vasculature than via the airways. Thus, we used a lipid-based cmRNA formulation (PLF) optimized for pulmonary delivery for intravenous application in mice. This formulation showed strong and selective protein translation in the lung (Figures 5A and 5B). Administration of PLF containing ACE2 cmRNA led to equally strong ACE2 protein translation in the lung (Figure 5C). Immunostainings showed that sham-treated animals expressed ACE2 in type II AECs as already observed by Wiener et al.,[66] while ACE2 cmRNA-treated lungs presumably also express ACE2 in type I AECs. These findings are especially valuable for therapeutic application in IPF; unlike rodent lungs, human lungs also express ACE2 in type I AECs,[67,68] rendering them an enormous pool for locally active ACE2 protein to break the vicious circle of AngII-stimulated ACE2 downregulation and apoptosis. Establishing ACE2 translation in type I AECs could not be achieved by recombinant protein therapy[21] or lentiviral-mediated *ACE2* overexpression.[23]

Figure 4. Liver-Targeted cmRNA Delivery

(A) Mice received 1 mg/kg luciferase cmRNA in LLF injected intravenously. 6 hr after injection, animals were euthanized and luminescence was determined for whole animals as well as for the liver, spleen, and lung. IVIS images of three representative animals are shown. (B) Organs were homogenized and luciferase activity was determined. For statistical analysis, the lung signal was compared pairwise to each other organ. (C) Part of the liver was embedded in paraffin and stained for luciferase protein with anti-luciferase antibody. The asterisk indicates the portal vessel, and the "x" indicates the central vein. Mice received 4 mg/kg and 2 mg/kg codon-optimized hαG ACE2 cmRNA or 2 mg/kg control cmRNA in LLF by intravenous injection. 6 hr after transfection, animals were euthanized and livers were excised. (D) Part of the liver was embedded in paraffin and in situ hybridization was performed for detection of ACE2 cmRNA (black signal) and endogenous ACE2 (pink signal). (E) For quantification of ACE2 cmRNA, total RNA was extracted and transcribed into first-strand cDNA. ACE2 cmRNA was quantified by real-time PCR. (F) Part of the liver was homogenized and analyzed by western blot. The upper panel shows a western blot detecting ACE2 protein for all treatment groups with GAPDH as the loading control. The cell lysate of ACE2 cmRNA-transfected hepatocytes was used as a positive control (p.c.). The lower panel is a western blot showing full deglycosylation of ACE2 protein in animals treated with 2 mg/kg ACE2 cmRNA. (G) ACE2 activity assay was performed for all groups. Organs were compared using the Student's t test, while the group comparison was done with one-way ANOVA. $^{**}p < 0.01$. FI, fluorescence intensity. Means ± SD are shown.

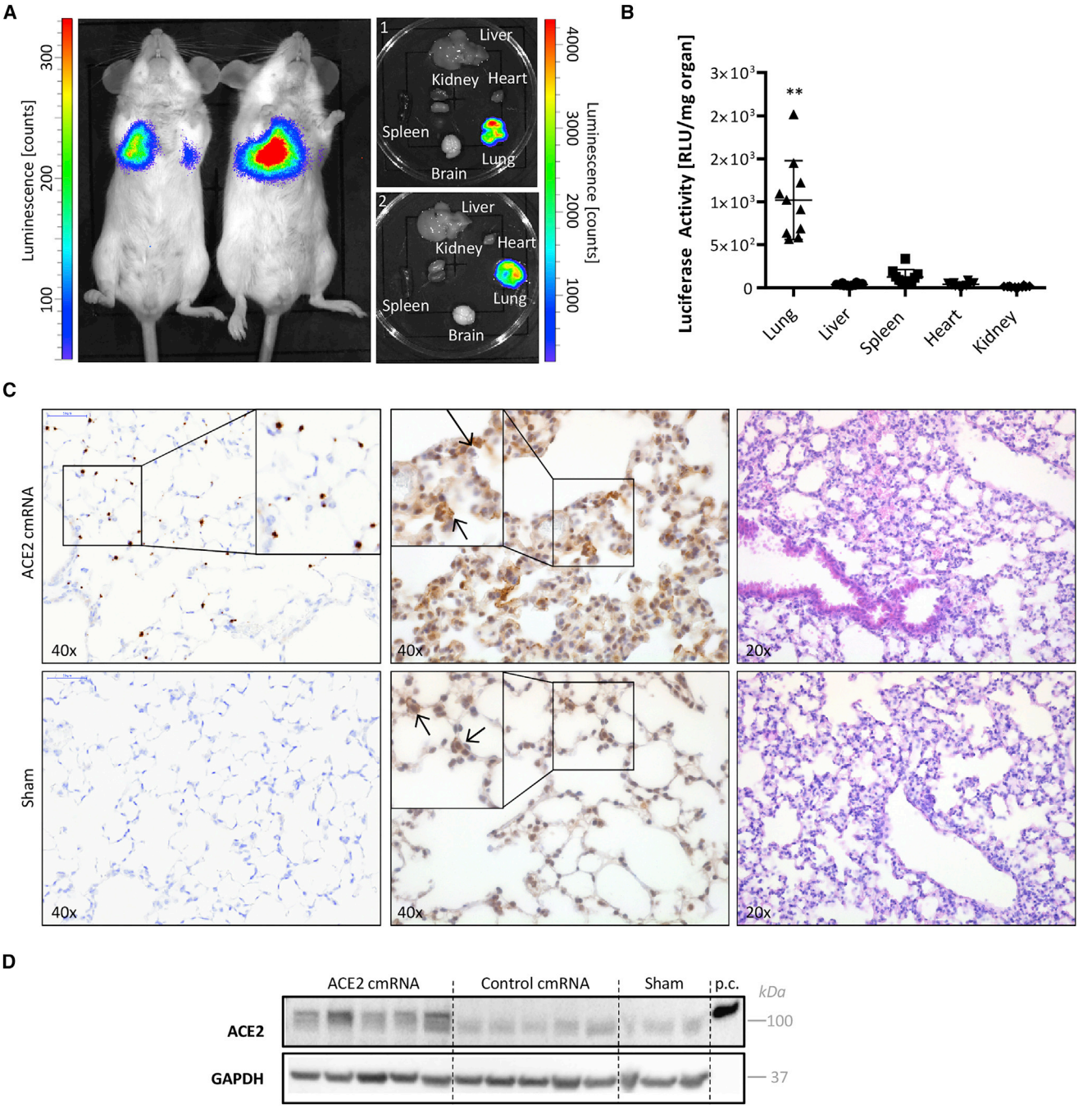

Figure 5. Lung-Targeted cmRNA Delivery

(A) Mice received 1 mg/kg luciferase cmRNA in PLF injected intravenously. Animals were euthanized 6 hr after treatment and luminescence was determined for two representative animals and selected organs. Codon-optimized hαG ACE2 and 10% luciferase cmRNA were formulated in PLF and administered intravenously at a dose of 1 mg/kg. (B) Organs were homogenized and luciferase activity was measured. For statistical analysis, the lung signal was compared pairwise to each other organ. (C) After the left lungs were embedded in paraffin, ACE2 cmRNA was visualized by in situ hybridization (left panel). Tissues were also stained for ACE2 protein, detected by anti-ACE2 antibody. Arrows highlight cells with ACE2 protein enrichment (middle panel). Hematoxylin staining of the lungs is shown (right panel). (D) Western blot of homogenized lung samples with GAPDH as the loading control. Means ± SD are shown.

In summary, we advanced the latest RNA technology for sustained local ACE2 translation in the liver or lung. These achievements highlight the strengths of RTT over recombinant protein therapy, where protein half-life,[33] immunogenicity,[69] and organ- or cell-targeted delivery are still challenging. Compared to non-viral gene transfer by pDNA, RTT shows strong translation efficiency without the risk of insertional mutagenesis,[25] a problem also found with retroviral, lentiviral, and adeno-associated gene transfer.[70] In addition, the time frame of viral-mediated gene expression is difficult to control, lasting up to years in the case of adeno-associated viruses.[70] Furthermore, in contrast to gene therapy, cell division is not needed for successful protein expression in RTT. In this study, we designed an ACE2 cmRNA sequence, leading to strong and stable ACE2 protein translation in vitro and in vivo. In combination with selected lipidoid and lipid nanoparticles serving as carrier systems, we were able to translate ACE2 protein selectively in the liver and lung, which may allow re-establishment of local RAS balance. Due to its self-limited translation without the risk of genomic integration, ACE2 protein translation can be fine-tuned to each patient's needs with a controllable treatment duration until the halt or resolution of fibrosis. Therefore, we consider ACE2-based RTT a promising approach for the treatment of liver and lung fibrosis to be tested in fibrotic disease models.

MATERIALS AND METHODS

cmRNA Preparation

Chemically modified mRNA was synthesized as previously described.[71] In brief, the respective pDNA templates were subjected to in vitro transcription using T7 RNA Polymerase (Thermo Fisher Scientific) with a predefined mix of natural and chemically modified ribonucleotides. To enhance RNA stability, a C1-m7G cap structure was enzymatically added at the 5′ end of the transcript, while the 3′ end was subjected to polyadenylation of ~ 200 nucleotides. The cmRNA product was purified by ammonium-acetate precipitation and was re-suspended in water at the desired concentration. Purity and quality were checked on a NanoDrop2000C spectrophotometer (Thermo Fisher Scientific) and with the Standard Sensitivity RNA Analysis Kit on a Fragment Analyzer (Advanced Analytical Technologies). The following cmRNA sequences were designed: human ACE2 5′ and 3′ UTRs (natural), GGGAGAC(Nat)GCCACCA TG____TGA(Nat)-poly(A); minimal 5′ UTR (minimal), GGGAGA CGCCACCATG____TGA-poly(A); human alpha globin 5′ UTR (hαG), GGGAGAC(hαG)GCCACCATG____TGA-poly(A); and human CYBA 5′ and 3′ UTR (CYBA), GGGAGAC(CYBA)GCCACCA TG____TGA(CYBA)-poly(A). The structure of the natural human ACE2 UTRs (Nat) was retrieved from NCBI GenBank (GenBank: NM_021804.2). The hαG 5′ UTR (hαG) was designed with omission of the first 30 nucleotides of the hαG reference sequence (GenBank: NM_000517.4) and introduction of an additional "G" to give a full Kozak element upstream of ATG. CYBA UTRs (CYBA) were designed as previously described.[41]

cmRNA Lipoplex Formation and Transfection

For in vitro experiments, lipoplexes were formed using an in-house transfection reagent, Lipofectamine 2000, or Lipofectamine MessengerMAX (Thermo Fisher Scientific) depending on the experimental aim and cell type. For the initial proof of concept, an in-house transfection reagent comprising preassembled C12-(2-3-2)/DPPC/cholesterol/DMG-PEG2k lipoplexes in aqueous solution was used at an N/P ratio (molar ratio of amino groups of lipid to phosphate groups of cmRNA) of 8. In brief, cmRNA in aqueous solution was rapidly injected into the appropriate amount of in-house transfection reagent, followed by 5-min incubation at room temperature (RT) for self-assembly of cmRNA and lipoplexes. Screening of the eight cmRNA sequences was performed using Lipofectamine 2000 (Thermo Fisher Scientific) as the transfection reagent, while primary cells were transfected with Lipofectamine MessengerMAX (Thermo Fisher Scientific). Transfection was carried out according to the manufacturer's protocol with a cmRNA-to-transfection reagent ratio of 1:2 for Lipofectamine 2000 and 1:1.5 for Lipofectamine MessengerMAX. In general, 2 μg cmRNA per well was used for experiments performed in six-well plates, 250 ng and 25 ng cmRNA per well for 24-well plates, and 16 ng cmRNA per well for 96-well plates. For all experiments, cells were seeded in a number to reach 70% confluence within 24 hr. After 24 hr, the medium was renewed and lipoplexes were added dropwise with or without 0.005 mg/mL tunicamycin (Sigma-Aldrich). The medium was replaced 4 hr after transfection for cells transfected with Lipofectamine MessengerMAX or after 24 hr if cells were kept in culture for more than 24 hr.

For liver-targeted in vivo experiments, cmRNA was formulated in LLF as previously described.[35] Lung-targeted lipoplexes (PLF) were prepared by mixing cmRNA with in-house polyethylene glycol (PEG) co-polymer in aqueous solution and applying it to a mix of preassembled lipid micelles. After incubation for 15 min at RT for self-assembly of cmRNA in this PLF, the mix was transferred into Dulbecco's PBS (Thermo Fisher Scientific) supplemented with 2% sucrose. Lipoplexes were applied in a final volume of 150 μL per animal with a cmRNA dose of 1 mg/kg.

Isolation and Cell Culture of Murine Liver and Lung Cells

Liver cells were isolated from 8-week-old male C57BL/6J mice. For hepatocyte isolation, animals were euthanized and the liver was perfused via the portal vein with EGTA buffer, which contained 25 mM HEPES (Gibco/Life Technologies), pH 8.5, 5.7 g/L glucose (Applichem), 103 mM NaCl, 2.4 mM KCl, 1.23 mM KH_2PO_4, 0.480 mM L-glutamine (Biochrome), 15% (v/v) amino acids (Sigma-Aldrich), and 0.5 mM EGTA. In the next step, hepatocytes were extracted by digestion of liver tissue with a collagenase solution, which contained 25 mM HEPES, pH 8.5, 5.7 g/L glucose, 103 mM NaCl, 2.4 mM KCl, 1.23 mM KH_2PO_4, 0.480 mM L-glutamine, 12% (v/v) amino acids, 2 mM $CaCl_2$, and 3.5 mM $MgCl_2$ supplemented with 0.12 U/mL type NB 4G collagenase (Serva), and they were subjected to a Percoll gradient (GE Healthcare). Cells were then seeded on Collagene R (Serva)-coated six-well plates in William's E medium (PAN-Biotech) supplemented with 0.22 mM L-glutamine, 0.02 M HEPES, pH 7.4, 0.5% penicillin/streptomycin (Biochrome), 100 mg/L gentamycin (Sigma-Aldrich), 110 nM hydrocortisone (RotexMedica), insulin (Novo Nordisk), 1.6% DMSO (Sigma-Aldrich), and 10% fetal calf

serum (FCS) (PAN-Biotech). After cell attachment, the medium was changed to culture medium supplemented with 1% FCS.

Fibroblast extraction was performed by excising lungs of 16-week-old C57BL/6J wild-type mice after an intraperitoneal overdose of ketamine/xylazine and cervical dislocation. Under sterile conditions, the lungs were flushed with PBS after cannulation of the right ventricle. The flushed lungs were then excised, diced into 2- to 3-mm pieces, and digested in media with collagenase solution, which contained DMEM/F-12, L-glutamine, and 15 mM HEPES (Gibco/Life Technologies) supplemented with 26.5 U/mL collagenase type I (Biochrome). The digested tissue was filtered, washed with PBS, and seeded in culture medium, which contained DMEM/F-12, L-glutamine, 15 mM HEPES, and 10% heat-inactivated FCS (Gibco/Life Technologies), and 1% penicillin/streptomycin (Gibco/Life Technologies). Experiments were performed between passages 4 and 6.

All cells were cultured in a humidified 5% CO_2 incubator at 37°C with an exchange of culture medium every 2–3 days.

Cell Culture of Human Cell Lines

A549 (ACC-107) and HEK293 (ACC-305) cells were purchased from DSMZ and cultured in minimum essential media (MEM) with GlutaMAX (Gibco/Life Technologies). HepG2 cells were purchased from DSMZ (ACC-180) and cultured in RPMI 1640 plus GlutaMAX (Gibco/Life Technologies). Within the 2 years of in vitro experiments, cross-contamination was checked by short tandem-repeat profiling. The medium for all three cell lines was supplemented with 10% heat-inactivated FCS (Gibco/Life Technologies) and 1% penicillin/streptomycin (Gibco/Life Technologies). Cells were cultured in a humidified 5% CO_2 incubator at 37°C. The cell culture medium for A549, HepG2, and HEK293 cells was renewed twice a week and cells were passaged at 80% confluence.

cmRNA Quantification and Relative Gene Expression Analysis

Total RNA was isolated from cell culture or tissue samples using the Nucleospin RNA Plus Kit (Machery-Nagel) and total RNA was transcribed into cDNA using the Transcriptor First-Strand cDNA Synthesis Kit (Roche Diagnostics). Real-time qPCR was performed with SsoAdvanced Universal SYBR Green Supermix (Bio-Rad) on a Roche Light Cycler 96 (Roche Diagnostics). The following primers were used: ACE2 cmRNA in vitro experiments (5′-ggccaatcactacg aggact-3′ and 5′-tccactccgttcacctcata-3′); native ACE2 cmRNA construct screen (5′-aaaaatgagatggcaagagca-3′ and 5′-gccatctaccccattt acttca-3′); codon-optimized ACE2 cmRNA construct screen (5′- aata cgtggtgctgaagaacg-3′ and 5′-agtcgccgtagtcctcgtag-3′); human ACE2 (5′-ccagtggatgaaaaagtggtg-3′ and 5′-gtttcatcatggggcacag-3′); human β-actin (PrimePCR SYBR Green Assay; Bio-Rad); human TATA-binding protein (PrimePCR SYBR Green Assay); human β-2-microglobulin (5′-ttctggcctggaggctatc-3′ and 5′-tcaggaaatttgactttccattc-3′); human mitochondrial ribosomal protein L19 (MRPL19) (5′-ggaatgtt atcgaaggacaagg-3′ and 5′-caggaagggcatctcgtaag-3′); human succinate dehydrogenase, subunit A (SDHA) (5′-tccactacatgacggagcag-3′ and 5′-ccatcttcagttctgctaaacg-3′); mouse ACE2 (5′-tgtagaacgtaccttcgc agag-3′ and 5′-gtaggaagggtaggtatccatcaa-3′); mouse hypoxanthine-guanine phosphoribosyltransferase (Hprt) (5′-ggagcggtagcacctcct-3′ and 5′-aacctggttcatcatcgctaa-3′); mouse MRPL19 (5′-cgagtacagcacc tttgacg-3′ and 5′-ggcttcattttaactttcagcttg-3′); mouse SDHA (5′-ttgagat ccgtgaaggaagag-3′ and 5′-tagacgtgtggccagttgc-3′; and mouse glucuronidase beta (Gusb) (PrimePCR SYBR Green Assay).

Reference genes used in Figure 1A were β-actin and TATA-box binding protein for human samples; MRPL19, Gusb, and SDHA for hepatocytes; and MRPL19 and HPRT for lung fibroblasts. Absolute cmRNA values were calculated by interpolation using GraphPad Prism software. Half-lives and 95% confidence intervals were calculated applying a one-phase exponential decay function with automatic outlier elimination in GraphPad Prism software.

Western Blot Analysis

For in vitro experiments, cells were lysed with 0.5% Triton X-100 in ACE2 lysis buffer (1 M NaCl, 0.5 mM $ZnCl_2$ and 75 mM Tris-HCl, pH 7.5), while ex vivo samples were lysed with RIPA buffer (50 mM Tris, pH 8.0, 150 mmol/L NaCl, 1.0% Triton X-100, 0.5% sodium deoxycholate, and 0.1% sodium dodecyl sulfate). Total protein content was determined by the bicinchoninic acid (BCA) assay, following the manufacturer's instructions (Thermo Fisher Scientific). If applicable, parts of the lysates were used for deglycosylation with NEB Protein Deglycosylation Mix II following the manufacturer's instructions for denaturing conditions (New England Biolabs). Cell lysates were separated on 8% or 4%–12% polyacrylamide gels (Thermo Fisher Scientific) and transferred to polyvinylidene fluoride (PVDF) membranes (Bio-Rad). Membranes were blocked in gelatin buffer (50 mM Tris, pH 7.5, 150 mM NaCl, 0.05% Triton X-100, 5 mM EDTA, and 0.25% gelatin) and probed with antibodies against ACE2 (0.1 μg/mL, AF933; R&D Systems/Bio-Techne) and glyceraldehyde-3-phosphate dehydrogenase (GAPDH) (1:10,000, 5174; Cell Signaling Technology/New England Biolabs). For protein detection, horseradish peroxidase (HRP)-conjugated anti-goat (1:10,000, sc2020) and anti-rabbit (1:10,000, sc2004; both from Santa Cruz Biotechnology) antibodies were added. For signal detection, Luminata Western HRP substrate was applied according to the manufacturer's protocol (Merck Chemicals).

ACE2 Activity Assay

To quantify ACE2 activity, cell culture samples were lysed as for western blotting. The ACE2 activity assay was adapted from Pedersen et al.[73] 30 μg total protein extract was incubated with or without DX600 (Bachem) for 20 min at RT in ACE2 reaction buffer. 10 μM synthetic substrate Mca-Y-V-A-D-A-P-K(Dnp)-OH (R&D Systems) was added to a total volume of 100 μL and incubated for at least 60 min at 37°C.

Ex vivo samples were prepared as described by Joyner et al.[72] In brief, frozen liver and lung samples were homogenized in ACE2 reaction buffer (Complete; Roche Diagnostics), which contained 25 nM HEPES buffer, 125 nM NaCl, and 10 μM $ZnCl_2$, pH 7.4, followed by a centrifugation at 2,500 × *g* for 5 min. The supernatant was collected and spun for 10 min at 28,000 × *g*. The resulting pellet

was re-suspended in reaction buffer before overnight incubation with 0.5% Triton X-100 at 4°C and gentle shaking. Samples were centrifuged for 5 min at 28,000 × *g*, the supernatant was collected, and the total protein content was measured by the BCA assay. For the assay, 20 μg protein was incubated for 20 min at RT in ACE2 reaction buffer containing 10 μM Captopril (Santa Cruz Biotechnology), an ACE inhibitor. 1 mM MLN4760 (Exclusive Chemistry), another ACE2 inhibitor, was added, followed by another incubation for 20 min at RT. Finally, 1 mM substrate Mca-A-P-K(DnP) (Caslo) was added and samples were incubated for 1 hr at 37°C.

Fluorescence of all samples was measured on a Tecan Infinite 200 PRO plate reader with excitation at 320 nm and emission at 405 nm.

Flow Cytometry Analysis

Correct protein integration into the plasma membrane was assessed by flow cytometry. Cells were washed with PBS, detached with TrypLE (Gibco/Life Technologies), and re-suspended in flow cytometry buffer (PBS supplemented with 10% FCS). Cells were incubated with primary antibody against ACE2 (5 μg/mL, AF933; R&D Systems) in flow cytometry buffer for 1 hr at 4°C. After washing with flow cytometry buffer, anti-goat AF488 antibody (1:400, A11087; Thermo Fisher Scientific) was added for 1 hr at 4°C. Cells were washed again in flow cytometry buffer and stained with propidium iodide for discrimination between live and dead cells (1 μg/mL Sigma-Aldrich). Analysis was performed on an Attune Acoustic Focusing Cytometer (Life Technologies) with Attune Cytometric Software (version 2.1; Life Technologies) and FlowJo (version 10).

Firefly Luciferase Assay

For detection of firefly luciferase activity, 60–90 mg frozen lung tissue was lysed in luciferase lysis buffer (25 mM Tris-HCl, 1% Triton X-100, and Complete). 100 μL luciferin substrate (0.47 mM D-luciferin, 0.27 mM coenzyme A, 33.3 mM 1,4-dithiothreitol, 0.53 mM ATP, 1.1 mM $MgCO_3$, 2.7 mM magnesium sulfate heptahydrate, 20 mM Tricine, and 0.1 mM EDTA disodium salt dihydrate) was added to the tissue homogenate and photon emission was measured for 1 s on a Lumat LB 9507 (Berthold Technologies).

In Vivo Bioluminescence Imaging

Mice were anesthetized, followed by a 3 mg intraperitoneal and 1.5 mg intra-nasal application of D-luciferin substrate (Synchem) dissolved in PBS at 30 mg/mL, pH 7.0. Bioluminescence was measured 10 min later using an IVIS Lumina XR Imaging System (Caliper Life Sciences) with an exposure time of 1 min. Organs were excised and placed on a Petri dish and reimaged on the IVIS system.

Animal Studies

Animal studies were performed in BALB/c or C57BL/6J mice. Animals were purchased from Charles River Laboratories, and they were 9–11 weeks of age and weighed ~20 g at the start of the experiment. All studies were approved by the Government of Upper Bavaria or by the Norddeutsches Landesamt für Verbraucherschutz und Lebensmittelsicherheit (LAVES) in Germany, and all animal experiments were carried out according to the guidelines of the German law of protection of animal life and reviewed by the local ethics committee.

Immunofluorescence Staining

Cells were cultured on coverslips in six-well plates. After washing with PBS, 20 μg/mL tetramethylrhodamine-conjugated wheat germ agglutinin (Thermo Fisher Scientific) in Hank's balanced salt solution (Gibco/Life Technologies) was added to the samples and incubated for 10 min in the incubator. Samples were washed with PBS and fixed in 4% paraformaldehyde for 10 min at RT. Cells were washed again and incubated for 10 min with 0.2% Triton X-100 at RT. After another washing step, cells were blocked in PBS supplemented with 10% FCS and 0.05% Triton X-100 for 30 min at RT. Slides were then incubated for 1 hr with primary antibody against ACE2 (5 μg/mL, AF933; R&D Systems) at RT, followed by another washing step. Secondary anti-goat AF488 antibody (1:400, A11087; Thermo Fisher Scientific) and DAPI (1 μg/mL; Sigma-Aldrich) were added and incubated for 1 hr at RT. After a final wash, slides were mounted in FluorSave (Merck Chemicals) and viewed under a Leica DMi8 microscope (Leica Microsystems).

Immunohistochemistry

Liver and lung tissues were excised, fixed for 24 hr in 4% buffered formaldehyde solution, and embedded in paraffin for histological examination. Tissues were then sectioned into 3- to 4-μm slices, deparaffinized, and rehydrated in a graded ethanol series. For antigen retrieval, tissue sections were incubated in 10 mM citrate buffer, pH 6.0, for 30 min using a waterbath at 96°C, washed in PBS, and quenched for 5 min in 3% H_2O_2. After another washing step, sections for luciferase were blocked for 1 hr at RT in 2.5% horse serum in PBS (Vector Laboratories). The sections were then incubated with primary anti-luciferase antibody (1:300, G7451; Promega) in PBS supplemented with 0.3% Triton X-100 at 4°C overnight. Tissue sections were washed in PBS and incubated with ImmPRESS reagent (Vector Laboratories) for 30 min at RT. After washing again with PBS, 3,3′-diaminobenzidine substrate at 0.5 mg/mL in PBS was added for 1–8 min at RT. For ACE2 staining, the tissue sections were additionally subjected to an avidin/biotin block (Vector Laboratories) for 15 min at RT, followed by a brief wash. Then tissues were blocked in Vectastain serum-blocking reagent D (Vector Laboratories) for 30 min at RT, followed by an overnight incubation at 4°C with primary anti-ACE2 antibody (10 μg/mL, AF933; R&D Systems) in 10% normal goat serum (Life Technologies) in PBS supplemented with 0.2% Triton X-100. After washing with PBS, the sections were incubated with Vectastain biotinylated anti-goat immunoglobulin G (IgG) (diluted according to the manufacturer's protocol; Vector Laboratories), washed again, and incubated with Vectastain ABC reagent (Vector Laboratories), each for 30 min at RT. 3,3′-diaminobenzidine substrate was added at 0.5 mg/mL in PBS for 1 min at RT and the reaction was stopped by washing tissue sections in distilled water. After a counterstaining with hematoxylin (Roth), sections were evaluated under a Leica DM2000 LED microscope (Leica Microsystems).

In Situ Hybridization

In situ hybridization of liver tissues was performed by Advanced Cell Diagnostics (ACD), while lung tissues were analyzed by ITEM using a brown RNAscope 2.5 HD Reagent Kit (catalog no. 322300; ACD) following the manufacturer's instructions. For detection of ACE2 cmRNA, a targeted probe was designed by ACD based on the cmRNA sequence provided, while a probe detecting murine ACE2 was derived from GenBank (Genbank: NM_027286.4) RNAscope dapB (bacterial *dap*B; ACD) was used as a negative control, and RNAscope PPIB (cyclophilin B; ACD) as a positive control. Samples were counterstained with hematoxylin and viewed under a bright-field microscope.

Statistical Analysis

Each experiment was performed with at least three technical replicates per sample. In addition, quantitative analysis of fluorescence-activated cell sorting (FACS) samples and screening for the best performing cmRNA construct was performed with a minimum of three biological replicates. Results are shown as means ± SD unless otherwise stated. Statistical analysis was performed using GraphPad Prism software (version 6). Pairwise comparison of in vitro experiments was conducted by the two-tailed Student's t test and group comparisons of in vivo experiments were done by one-way ANOVA, followed by the Dunnett multiple-comparisons test. A p value ≤ 0.05 was considered statistically significant.

SUPPLEMENTAL INFORMATION

Supplemental Information includes eight figures and can be found with this article online at http://dx.doi.org/10.1016/j.omtn.2017.04.006.

AUTHOR CONTRIBUTIONS

E.S. performed proof-of-concept in vitro studies and M.H. executed the screen of ACE2 cmRNA sequences. D.W. provided primary murine hepatocytes, while A.H. and P.O. provided primary murine lung fibroblasts. J.G. and M.A. designed and produced cmRNA. C.D. and O.M. provided lipoplex formation for the in vivo experiments. G.H., T.P., and A.H.-J. conducted the animal experiments, while E.S. performed the ex vivo assays; V.K. coordinated the histological analysis and D.E. performed the pathologic evaluation of tissues. H.-G.H. and D.S. performed in situ hybridization of lung tissues. R.K.-D., C.P., and C.R. supervised the project and refined the manuscript; E.S. performed the data analysis and wrote the manuscript.

CONFLICTS OF INTEREST

M.H., M.A., C.D., D.E., J.G., G.H., A.H.-J., V.K., R.K.-D., O.M., and T.P. are employees of Ethris GmbH, and C.R. and C.P. hold equity in Ethris GmbH.

ACKNOWLEDGMENTS

The laboratory work was done at Ethris GmbH, the Institute of Lung Biology and Disease (Helmholtz Zentrum Munich), and the Institute of Molecular Immunology and Experimental Oncology. This study was supported by the Biochance project (031A526) funded by the Federal Ministry of Education and Research (BMBF) and Deutsche Forschungsgemeinschaft (DFG) via the Nanosystems Initiative Munich (NIM) Excellence Cluster. We thank all members of Ethris GmbH for technical support and discussions. We acknowledge Jana Lambrecht for contributions with regard to PKR activation, Katrin Lindner for support in histological processing of in vivo samples, and Philipp Beck for help with the setup of the ACE2 activity assay.

REFERENCES

1. Wynn, T.A., and Ramalingam, T.R. (2012). Mechanisms of fibrosis: therapeutic translation for fibrotic disease. Nat. Med. *18*, 1028–1040.
2. Rosenbloom, J., Mendoza, F.A., and Jimenez, S.A. (2013). Strategies for anti-fibrotic therapies. Biochim Biophys Acta *1832*, 1088–1103.
3. Liedtke, C., Luedde, T., Sauerbruch, T., Scholten, D., Streetz, K., Tacke, F., Tolba, R., Trautwein, C., Trebicka, J., and Weiskirchen, R. (2013). Experimental liver fibrosis research: update on animal models, legal issues and translational aspects. Fibrogenesis Tissue Repair *6*, 19.
4. Funke, M., and Geiser, T. (2015). Idiopathic pulmonary fibrosis: the turning point is now! Swiss Med. Wkly. *145*, w14139.
5. Wynn, T.A. (2008). Cellular and molecular mechanisms of fibrosis. J. Pathol. *214*, 199–210.
6. Almeda-Valdes, P., Aguilar Olivos, N.E., Barranco-Fragoso, B., Uribe, M., and Méndez-Sánchez, N. (2015). The role of dendritic cells in fibrosis progression in nonalcoholic fatty liver disease. BioMed Res. Int. *2015*, 768071.
7. Raghu, G., Collard, H.R., Egan, J.J., Martinez, F.J., Behr, J., Brown, K.K., Colby, T.V., Cordier, J.F., Flaherty, K.R., Lasky, J.A., et al.; ATS/ERS/JRS/ALAT Committee on Idiopathic Pulmonary Fibrosis (2011). An official ATS/ERS/JRS/ALAT statement: idiopathic pulmonary fibrosis: evidence-based guidelines for diagnosis and management. Am. J. Respir. Crit. Care Med. *183*, 788–824.
8. Margaritopoulos, G.A., Vasarmidi, E., and Antoniou, K.M. (2016). Pirfenidone in the treatment of idiopathic pulmonary fibrosis: an evidence-based review of its place in therapy. Core Evidence *11*, 11–22.
9. Rogliani, P., Calzetta, L., Cavalli, F., Matera, M.G., and Cazzola, M. (2016). Pirfenidone, nintedanib and N-acetylcysteine for the treatment of idiopathic pulmonary fibrosis: A systematic review and meta-analysis. Pulm. Pharmacol. Ther. *40*, 95–103.
10. Koyama, Y., Xu, J., Liu, X., and Brenner, D.A. (2016). New developments on the treatment of liver fibrosis. Dig. Dis. *34*, 589–596.
11. Marshall, R.P., McAnulty, R.J., and Laurent, G.J. (2000). Angiotensin II is mitogenic for human lung fibroblasts via activation of the type 1 receptor. Am. J. Respir. Crit. Care Med. *161*, 1999–2004.
12. Marshall, R.P., Gohlke, P., Chambers, R.C., Howell, D.C., Bottoms, S.E., Unger, T., McAnulty, R.J., and Laurent, G.J. (2004). Angiotensin II and the fibroproliferative response to acute lung injury. Am. J. Physiol. Lung Cell. Mol. Physiol. *286*, L156–L164.
13. Clarke, N.E., and Turner, A.J. (2012). Angiotensin-converting enzyme 2: the first decade. Int. J. Hypertens. *2012*, 307315.
14. Lubel, J.S., Herath, C.B., Tchongue, J., Grace, J., Jia, Z., Spencer, K., Casley, D., Crowley, P., Sievert, W., Burrell, L.M., and Angus, P.W. (2009). Angiotensin-(1-7), an alternative metabolite of the renin-angiotensin system, is up-regulated in human liver disease and has antifibrotic activity in the bile-duct-ligated rat. Clin. Sci. *117*, 375–386.
15. Osterreicher, C.H., Taura, K., De Minicis, S., Seki, E., Penz-Osterreicher, M., Kodama, Y., Kluwe, J., Schuster, M., Oudit, G.Y., Penninger, J.M., and Brenner, D.A. (2009). Angiotensin-converting-enzyme 2 inhibits liver fibrosis in mice. Hepatology *50*, 929–938.
16. Mak, K.Y., Chin, R., Cunningham, S.C., Habib, M.R., Torresi, J., Sharland, A.F., Alexander, I.E., Angus, P.W., and Herath, C.B. (2015). ACE2 therapy using adeno-associated viral vector inhibits liver fibrosis in mice. Mol. Ther. *23*, 1434–1443.
17. Warner, F.J., Lubel, J.S., McCaughan, G.W., and Angus, P.W. (2007). Liver fibrosis: a balance of ACEs? Clin. Sci. *113*, 109–118.

18. Moreno, M., Gonzalo, T., Kok, R.J., Sancho-Bru, P., van Beuge, M., Swart, J., Prakash, J., Temming, K., Fondevila, C., Beljaars, L., et al. (2010). Reduction of advanced liver fibrosis by short-term targeted delivery of an angiotensin receptor blocker to hepatic stellate cells in rats. Hepatology *51*, 942–952.

19. Corey, K.E., Shah, N., Misdraji, J., Abu Dayyeh, B.K., Zheng, H., Bhan, A.K., and Chung, R.T. (2009). The effect of angiotensin-blocking agents on liver fibrosis in patients with hepatitis C. Liver Int. *29*, 748–753.

20. Li, X., Molina-Molina, M., Abdul-Hafez, A., Uhal, V., Xaubet, A., and Uhal, B.D. (2008). Angiotensin converting enzyme-2 is protective but downregulated in human and experimental lung fibrosis. Am. J. Physiol. Lung Cell. Mol. Physiol. *295*, L178–L185.

21. Wang, L., Wang, Y., Yang, T., Guo, Y., and Sun, T. (2015). Angiotensin-converting enzyme 2 attenuates bleomycin-induced lung fibrosis in mice. Cell. Physiol. Biochem. *36*, 697–711.

22. Rey-Parra, G.J., Vadivel, A., Coltan, L., Hall, A., Eaton, F., Schuster, M., Loibner, H., Penninger, J.M., Kassiri, Z., Oudit, G.Y., and Thébaud, B. (2012). Angiotensin converting enzyme 2 abrogates bleomycin-induced lung injury. J. Mol. Med. (Berl.) *90*, 637–647.

23. Shenoy, V., Ferreira, A.J., Qi, Y., Fraga-Silva, R.A., Díez-Freire, C., Dooies, A., Jun, J.Y., Sriramula, S., Mariappan, N., Pourang, D., et al. (2010). The angiotensin-converting enzyme 2/angiogenesis-(1-7)/Mas axis confers cardiopulmonary protection against lung fibrosis and pulmonary hypertension. Am. J. Respir. Crit. Care Med. *182*, 1065–1072.

24. Tavernier, G., Andries, O., Demeester, J., Sanders, N.N., De Smedt, S.C., and Rejman, J. (2011). mRNA as gene therapeutic: how to control protein expression. J. Control. Release *150*, 238–247.

25. Yamamoto, A., Kormann, M., Rosenecker, J., and Rudolph, C. (2009). Current prospects for mRNA gene delivery. Eur. J. Pharm. Biopharm. *71*, 484–489.

26. Sahin, U., Karikó, K., and Türeci, Ö. (2014). mRNA-based therapeutics–developing a new class of drugs. Nat. Rev. Drug Discov. *13*, 759–780.

27. Karikó, K., Kuo, A., and Barnathan, E. (1999). Overexpression of urokinase receptor in mammalian cells following administration of the in vitro transcribed encoding mRNA. Gene Ther. *6*, 1092–1100.

28. Stepinski, J., Waddell, C., Stolarski, R., Darzynkiewicz, E., and Rhoads, R.E. (2001). Synthesis and properties of mRNAs containing the novel "anti-reverse" cap analogs 7-methyl(3′-O-methyl)GpppG and 7-methyl (3′-deoxy)GpppG. RNA *7*, 1486–1495.

29. Gustafsson, C., Govindarajan, S., and Minshull, J. (2004). Codon bias and heterologous protein expression. Trends Biotechnol. *22*, 346–353.

30. Karikó, K., Buckstein, M., Ni, H., and Weissman, D. (2005). Suppression of RNA recognition by Toll-like receptors: the impact of nucleoside modification and the evolutionary origin of RNA. Immunity *23*, 165–175.

31. Karikó, K., Muramatsu, H., Welsh, F.A., Ludwig, J., Kato, H., Akira, S., and Weissman, D. (2008). Incorporation of pseudouridine into mRNA yields superior nonimmunogenic vector with increased translational capacity and biological stability. Mol. Ther. *16*, 1833–1840.

32. Apeiron Biologics. (2009). Safety and Tolerability Study of APN01 (Recombinant Human Angiotensin Converting Enzyme 2). ClinicalTrials.gov identifier NCT00886353. https://clinicaltrials.gov/ct2/show/study/NCT00886353?term=Apeiron&rank=2.

33. Haschke, M., Schuster, M., Poglitsch, M., Loibner, H., Salzberg, M., Bruggisser, M., Penninger, J., and Krähenbühl, S. (2013). Pharmacokinetics and pharmacodynamics of recombinant human angiotensin-converting enzyme 2 in healthy human subjects. Clin. Pharmacokinet. *52*, 783–792.

34. Kaczmarek, J.C., Patel, A.K., Kauffman, K.J., Fenton, O.S., Webber, M.J., Heartlein, M.W., DeRosa, F., and Anderson, D.G. (2016). Polymer-lipid nanoparticles for systemic delivery of mRNA to the lungs. Angew. Chem. Int. Ed. Engl. *55*, 13808–13812.

35. Jarzębińska, A., Pasewald, T., Lambrecht, J., Mykhaylyk, O., Kümmerling, L., Beck, P., Hasenpusch, G., Rudolph, C., Plank, C., and Dohmen, C. (2016). A single methylene group in oligoalkylamine-based cationic polymers and lipids promotes enhanced mRNA delivery. Angew. Chem. Int. Ed. Engl. *55*, 9591–9595.

36. Fenton, O.S., Kauffman, K.J., McClellan, R.L., Appel, E.A., Dorkin, J.R., Tibbitt, M.W., Heartlein, M.W., DeRosa, F., Langer, R., and Anderson, D.G. (2016). Bioinspired alkenyl amino alcohol ionizable lipid materials for highly potent in vivo mRNA delivery. Adv. Mater. *28*, 2939–2943.

37. Tipnis, S.R., Hooper, N.M., Hyde, R., Karran, E., Christie, G., and Turner, A.J. (2000). A human homolog of angiotensin-converting enzyme. Cloning and functional expression as a captopril-insensitive carboxypeptidase. J. Biol. Chem. *275*, 33238–33243.

38. Lambert, D.W., Yarski, M., Warner, F.J., Thornhill, P., Parkin, E.T., Smith, A.I., Hooper, N.M., and Turner, A.J. (2005). Tumor necrosis factor-alpha convertase (ADAM17) mediates regulated ectodomain shedding of the severe-acute respiratory syndrome-coronavirus (SARS-CoV) receptor, angiotensin-converting enzyme-2 (ACE2). J. Biol. Chem. *280*, 30113–30119.

39. Powell, L.D. (2001). Inhibition of N-linked glycosylation. Curr. Protoc. Immunol. *8*, 8.14.1–8.14.9.

40. Holtkamp, S., Kreiter, S., Selmi, A., Simon, P., Koslowski, M., Huber, C., Türeci, O., and Sahin, U. (2006). Modification of antigen-encoding RNA increases stability, translational efficacy, and T-cell stimulatory capacity of dendritic cells. Blood *108*, 4009–4017.

41. Ferizi, M., Leonhardt, C., Meggle, C., Aneja, M.K., Rudolph, C., Plank, C., and Rädler, J.O. (2015). Stability analysis of chemically modified mRNA using micropattern-based single-cell arrays. Lab Chip *15*, 3561–3571.

42. Babendure, J.R., Babendure, J.L., Ding, J., and Tsien, R.Y. (2006). Control of mammalian translation by mRNA structure near caps. RNA *12*, 851–861.

43. Qadah, T.H. (2014). A study of molecular mechanisms regulating human alpha globin production: an in vitro comparative study between normal and α-thalassemia subtypes. PhD thesis (Perth: University of Western Australia).

44. Bataller, R., Sancho-Bru, P., Ginès, P., Lora, J.M., Al-Garawi, A., Solé, M., Colmenero, J., Nicolás, J.M., Jiménez, W., Weich, N., et al. (2003). Activated human hepatic stellate cells express the renin-angiotensin system and synthesize angiotensin II. Gastroenterology *125*, 117–125.

45. Huang, Q., Xie, Q., Shi, C.C., Xiang, X.G., Lin, L.Y., Gong, B.D., Zhao, G.D., Wang, H., and Jia, N.N. (2009). Expression of angiotensin-converting enzyme 2 in CCL4-induced rat liver fibrosis. Int. J. Mol. Med. *23*, 717–723.

46. Min, F., Gao, F., Li, Q., and Liu, Z. (2015). Therapeutic effect of human umbilical cord mesenchymal stem cells modified by angiotensin-converting enzyme 2 gene on bleomycin-induced lung fibrosis injury. Mol. Med. Rep. *11*, 2387–2396.

47. Brown, N.J., and Vaughan, D.E. (1998). Angiotensin-converting enzyme inhibitors. Circulation *97*, 1411–1420.

48. Bader, M., Santos, R.A., Unger, T., and Steckelings, U.M. (2012). New therapeutic pathways in the RAS. J. Renin Angiotensin Aldosterone Syst. *13*, 505–508.

49. Jiang, F., Yang, J., Zhang, Y., Dong, M., Wang, S., Zhang, Q., Liu, F.F., Zhang, K., and Zhang, C. (2014). Angiotensin-converting enzyme 2 and angiotensin 1-7: novel therapeutic targets. Nat. Rev. Cardiol. *11*, 413–426.

50. Mauro, V.P., and Chappell, S.A. (2014). A critical analysis of codon optimization in human therapeutics. Trends Mol. Med. *20*, 604–613.

51. Marin, M. (2008). Folding at the rhythm of the rare codon beat. Biotechnol. J. *3*, 1047–1057.

52. Vallazza, B., Petri, S., Poleganov, M.A., Eberle, F., Kuhn, A.N., and Sahin, U. (2015). Recombinant messenger RNA technology and its application in cancer immunotherapy, transcript replacement therapies, pluripotent stem cell induction, and beyond. Wiley Interdiscip. Rev. RNA *6*, 471–499.

53. Pesole, G., Grillo, G., Larizza, A., and Liuni, S. (2000). The untranslated regions of eukaryotic mRNAs: structure, function, evolution and bioinformatic tools for their analysis. Brief. Bioinform. *1*, 236–249.

54. Pestova, T.V., Lorsch, J.R., and Hellen, C.U.T. (2007). The mechanism of translation initiation in eukaryotes. In Translational Control in Biology and Medicine, M.B. Mathews, N. Sonenberg, and J.W.B. Hershey, eds. (Cold Spring Harbor Laboratory Press), pp. 87–128.

55. Huang, Y., Cheng, Q., Ji, J.L., Zheng, S., Du, L., Meng, L., Wu, Y., Zhao, D., Wang, X., Lai, L., et al. (2016). Pharmacokinetic behaviors of intravenously administered siRNA in glandular tissues. Theranostics *6*, 1528–1541.

56. Wang, J., Lu, Z., Wientjes, M.G., and Au, J.L.-S. (2010). Delivery of siRNA therapeutics: barriers and carriers. AAPS J. *12*, 492–503.

57. Lorenzer, C., Dirin, M., Winkler, A.M., Baumann, V., and Winkler, J. (2015). Going beyond the liver: progress and challenges of targeted delivery of siRNA therapeutics. J. Control. Release *203*, 1–15.

58. Matsui, A., Uchida, S., Ishii, T., Itaka, K., and Kataoka, K. (2015). Messenger RNA-based therapeutics for the treatment of apoptosis-associated diseases. Sci. Rep. *5*, 15810.

59. Akinc, A., Querbes, W., De, S., Qin, J., Frank-Kamenetsky, M., Jayaprakash, K.N., Jayaraman, M., Rajeev, K.G., Cantley, W.L., Dorkin, J.R., et al. (2010). Targeted delivery of RNAi therapeutics with endogenous and exogenous ligand-based mechanisms. Mol. Ther. *18*, 1357–1364.

60. Dancer, R.C., Wood, A.M., and Thickett, D.R. (2011). Metalloproteinases in idiopathic pulmonary fibrosis. Eur. Respir. J. *38*, 1461–1467.

61. Wang, R., Zagariya, A., Ang, E., Ibarra-Sunga, O., and Uhal, B.D. (1999). Fas-induced apoptosis of alveolar epithelial cells requires ANG II generation and receptor interaction. Am. J. Physiol. *277*, L1245–L1250.

62. Wang, R., Zagariya, A., Ibarra-Sunga, O., Gidea, C., Ang, E., Deshmukh, S., Chaudhary, G., Baraboutis, J., Filippatos, G., and Uhal, B.D. (1999). Angiotensin II induces apoptosis in human and rat alveolar epithelial cells. Am. J. Physiol. *276*, L885–L889.

63. Li, X., Zhang, H., Soledad-Conrad, V., Zhuang, J., and Uhal, B.D. (2003). Bleomycin-induced apoptosis of alveolar epithelial cells requires angiotensin synthesis de novo. Am. J. Physiol. Lung Cell. Mol. Physiol. *284*, L501–L507.

64. Cosgrove, G.P., Brown, K.K., Schiemann, W.P., Serls, A.E., Parr, J.E., Geraci, M.W., Schwarz, M.I., Cool, C.D., and Worthen, G.S. (2004). Pigment epithelium-derived factor in idiopathic pulmonary fibrosis: a role in aberrant angiogenesis. Am. J. Respir. Crit. Care Med. *170*, 242–251.

65. Farkas, L., Gauldie, J., Voelkel, N.F., and Kolb, M. (2011). Pulmonary hypertension and idiopathic pulmonary fibrosis: a tale of angiogenesis, apoptosis, and growth factors. Am. J. Respir. Cell Mol. Biol. *45*, 1–15.

66. Wiener, R.S., Cao, Y.X., Hinds, A., Ramirez, M.I., and Williams, M.C. (2007). Angiotensin converting enzyme 2 is primarily epithelial and is developmentally regulated in the mouse lung. J. Cell. Biochem. *101*, 1278–1291.

67. Hamming, I., Timens, W., Bulthuis, M.L., Lely, A.T., Navis, G., and van Goor, H. (2004). Tissue distribution of ACE2 protein, the functional receptor for SARS coronavirus. A first step in understanding SARS pathogenesis. J. Pathol. *203*, 631–637.

68. Ren, X., Glende, J., Al-Falah, M., de Vries, V., Schwegmann-Wessels, C., Qu, X., Tan, L., Tschernig, T., Deng, H., Naim, H.Y., and Herrler, G. (2006). Analysis of ACE2 in polarized epithelial cells: surface expression and function as receptor for severe acute respiratory syndrome-associated coronavirus. J. Gen. Virol. *87*, 1691–1695.

69. Baker, M.P., Reynolds, H.M., Lumicisi, B., and Bryson, C.J. (2010). Immunogenicity of protein therapeutics: The key causes, consequences and challenges. Self Nonself *1*, 314–322.

70. Kotterman, M.A., Chalberg, T.W., and Schaffer, D.V. (2015). Viral vectors for gene therapy: translational and clinical outlook. Annu. Rev. Biomed. Eng. *17*, 63–89.

71. Kormann, M.S.D., Hasenpusch, G., Aneja, M.K., Nica, G., Flemmer, A.W., Herber-Jonat, S., Huppmann, M., Mays, L.E., Illenyi, M., Schams, A., et al. (2011). Expression of therapeutic proteins after delivery of chemically modified mRNA in mice. Nat. Biotechnol. *29*, 154–157.

72. Joyner, J., Neves, L.A., Granger, J.P., Alexander, B.T., Merrill, D.C., Chappell, M.C., Ferrario, C.M., Davis, W.P., and Brosnihan, K.B. (2007). Temporal-spatial expression of ANG-(1-7) and angiotensin-converting enzyme 2 in the kidney of normal and hypertensive pregnant rats. Am. J. Physiol. Regul. Integr. Comp. Physiol. *293*, R169–R177.

73. Pedersen, K.B., Sriramula, S., Chhabra, K.H., Xia, H., and Lazartigues, E. (2011). Species-specific inhibitor sensitivity of angiotensin-converting enzyme 2 (ACE2) and its implications for ACE2 activity assay. Am. J. Physiol. Regul. Integr. Comp. Physiol. *301*, R1293–R1299.

OMTN, Volume *7*

Supplemental Information

Translation of Angiotensin-Converting Enzyme 2 upon Liver- and Lung-Targeted Delivery of Optimized Chemically Modified mRNA

Eva Schrom, Maja Huber, Manish Aneja, Christian Dohmen, Daniela Emrich, Johannes Geiger, Günther Hasenpusch, Annika Herrmann-Janson, Verena Kretzschmann, Olga Mykhailyk, Tamara Pasewald, Prajakta Oak, Anne Hilgendorff, Dirk Wohlleber, Heinz-Gerd Hoymann, Dirk Schaudien, Christian Plank, Carsten Rudolph, and Rebekka Kubisch-Dohmen

S1

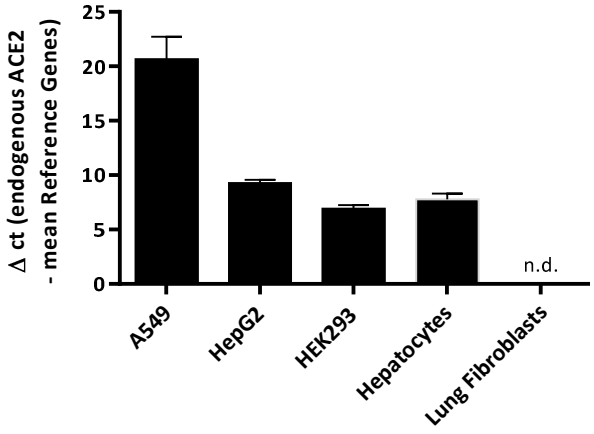

Figure S1. Levels of endogenous ACE2 mRNA. Total RNA of untreated cells of A549, HepG2 and HEK293 was collected and transcribed into first-strand cDNA. Real-time PCR was performed and delta ct values were calculated against a panel of reference genes. Reference genes for human cells: β-2-microglobulin, MRPL19 and SDHA. Reference genes for murine cells: MRPL19, GusB and HPRT.

S2

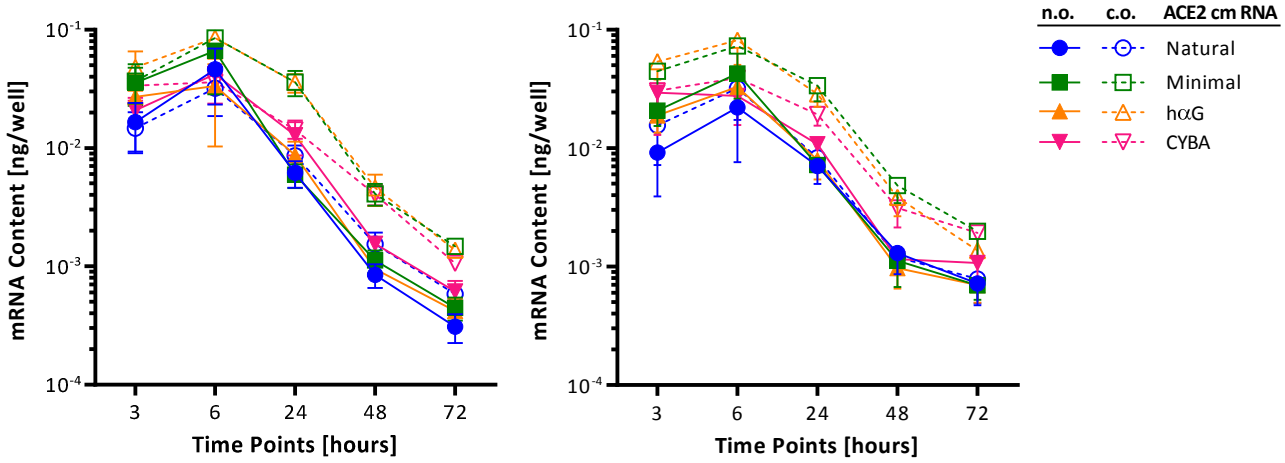

Figure S2. Kinetics of ACE2 cmRNA constructs in A549 and HepG2. A549 (left panel) and HepG2 (right panel) were lysed at time points indicated after transfection. Total RNA was collected and transcribed into first-strand cDNA. The amount of ACE2 cmRNA was quantified by real-time PCR.

S3

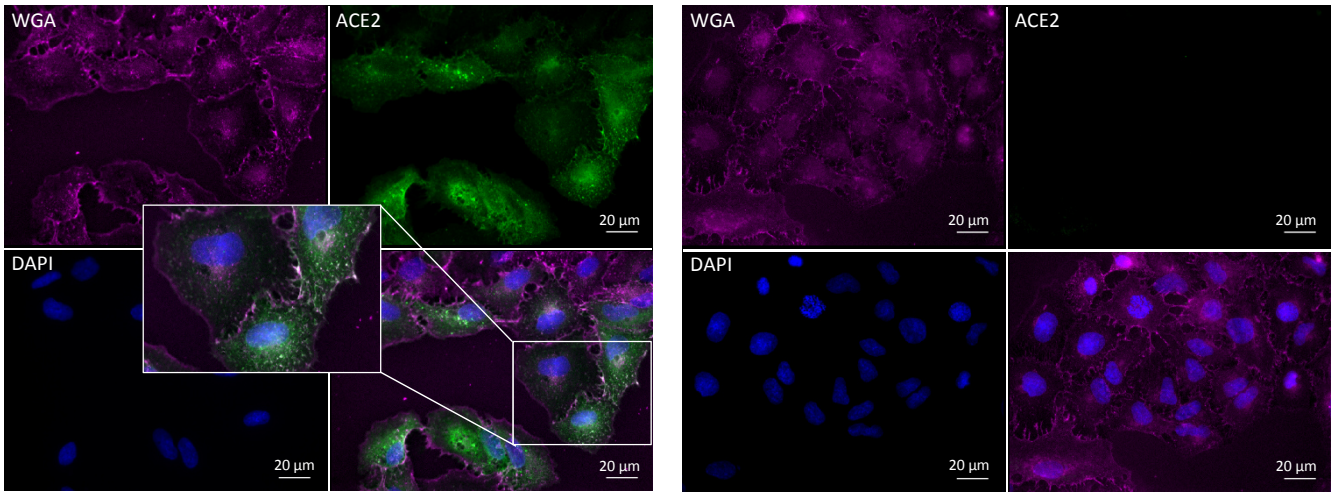

Figure S3. Immunofluorescent staining for ACE2 protein in A549. 24 h after transfection cells were incubated with tetramethyl-rhodamine conjugated wheat germ agglutinin for membrane staining, fixed and then stained with anti-ACE2 antibody (R&D Systems, 5 µg/ml, AF933). Finally, cell nuclei were stained with DAPI and ACE2 was visualized by addition of secondary anti-goat AF488 antibody (Thermo Fisher Scientific, 1:400, A11087). ACE2 cmRNA transfected cells (left panel) and control cmRNA transfected cells (right panel). green: ACE2, blue: nucleus, violet: cell membrane.

S4

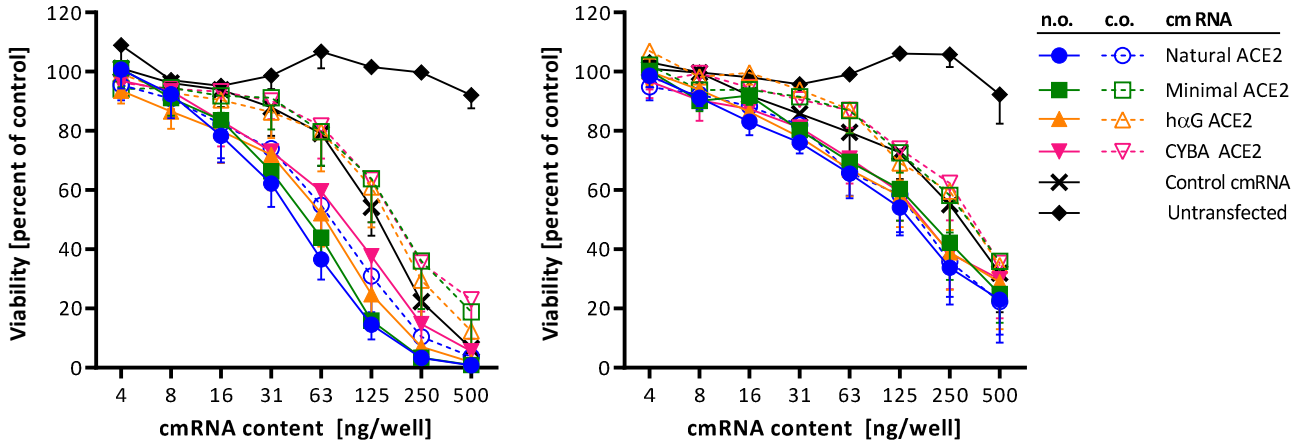

Figure S4. Viability of cells 72 h post cmRNA transfection. A549 (left panel) and HepG2 (right panel) were transfected with a decreasing series of metridia luciferase cmRNA. 72 h post transfection, cell supernatant was collected and luciferase activity was detected by addition of coelenterazine buffer (Synchem) and luminescence measurement on a Tecan Infinite 200 PRO plate reader.

S5

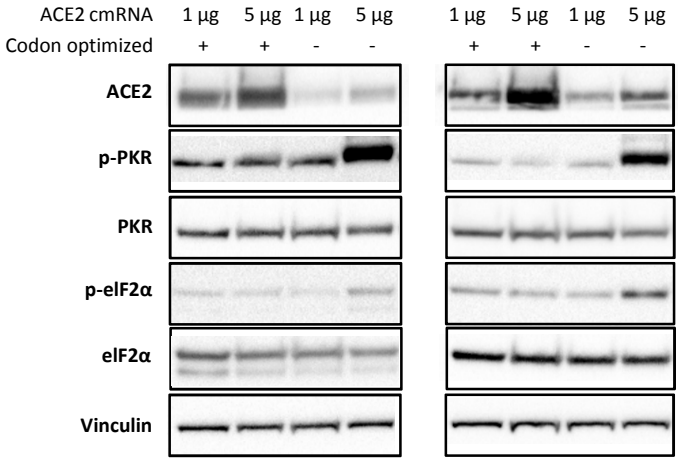

Figure S5. Effects of codon optimization on PKR activation. A549 (left panel) and HEK293 (right panel) were transfected with 1 or 5 µg of native or codon optimized hαG ACE2 cmRNA. 24 h after transfection, cells were lysed and cell lysate was analyzed by Western Blot with Vincullin as loading control. The following primary antibodies were used: anti-ACE2 (R&D systems, 0.1 µg/ml, AF933), anti – phospho eIF2α (Cell Signaling, 1:3000, #3398, detects phosphorylation on Ser51), anti-eIF2α (Cell Signaling, 1:3000, #2103), anti – phospho PKR (abcam, 1:3000, ab32036, detects phosphorylation on Thr446), anti-PKR (Cell Signaling, 1:3000, #12297), anti-Vinculin (abcam, 1:10000, ab91459). Secondary antibodies were used as previously described.

S6

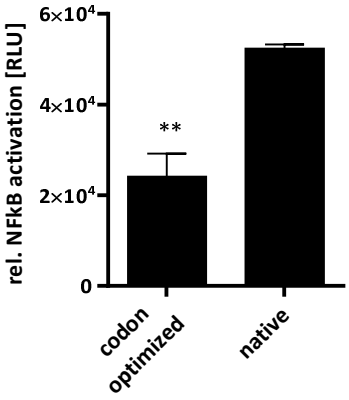

Figure S6. Effects of codon optimization on NFkB activation. NFkB activation was studied in HEK293 NFkB-reporter cells, which contain a luciferase gene under the control of a promoter with multiple Nuclear Factor-κB response elements. Upon binding of NFkB to the response elements, these cells express luciferase which can be detected by a luciferase activity assay. Cells were transfected with native or codon optimized hαG ACE2 cmRNA and lysed 24 h after transfection. Luciferase activity was then determined for the cell lsyates, which correlates to NFkB activation in these cells.

S7

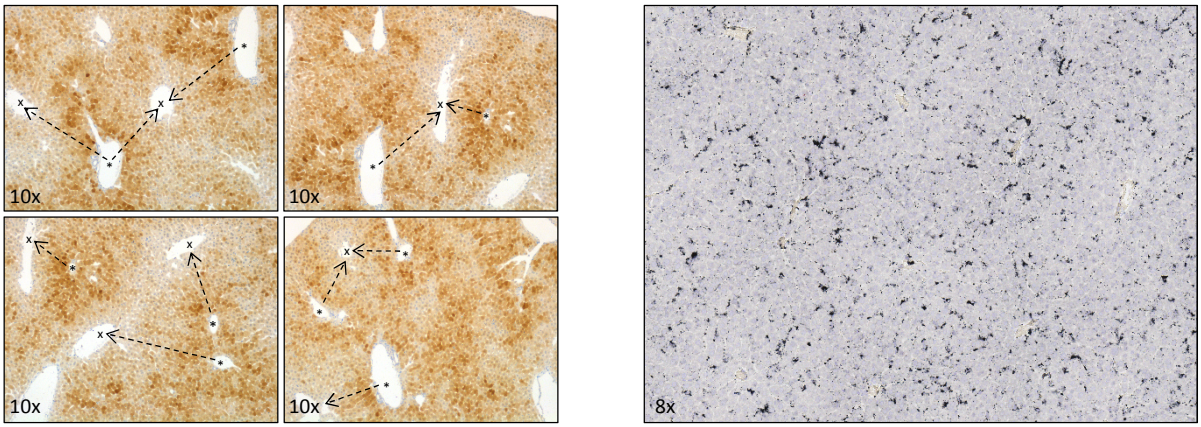

Figure S7. Left panel: Mice were intravenously injected 1 mg/kg of luciferase cmRNA in LLF. 6 h after injection, animals were sacrificed and parts of the liver was embedded in paraffin and stained for luciferase protein with anti-luciferase antibody. 4 representative images of luciferase cmRNA treated animals. * portal vessel, x central vein. Right panel: Mice received 4 mg/kg codon-optimized hαG ACE2 cmRNA in LLF by intravenous injection. 6 h after transfection, animals were sacrificed, liver excised and embedded in paraffin. In situ hybridisation was performed for detection of ACE2 cmRNA (black signal).

S8

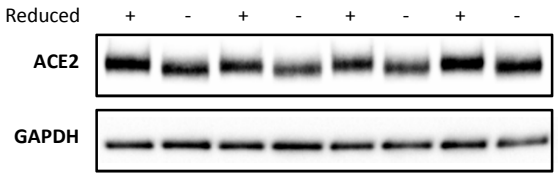

Figure S8. Disulfide bridge formation during posttranslational modification. A549 were transfected with 2 µg ACE2 cmRNA. 24 h after transfection, cells were lysed and cell lysate was analyzed by Western Blot under reducing and non-reducing conditions with GAPDH as loading control. The following primary antibodies were used: anti-ACE2 (R&D systems, 0.1 µg/ml, AF933), anti – GAPDH (Cell Signaling, 1:10000, #5174). Secondary antibodies were used as previously described. The same sample was applied repeatedly.